Available online at www.sciencedirect.com

ScienceDirect

Nuclear Physics B 920 (2017) 565–600

NUCLEAR PHYSICS B

www.elsevier.com/locate/nuclphysb

Thermal phase transition with full 2-loop effective potential

M. Laine *, M. Meyer, G. Nardini

AEC, Institute for Theoretical Physics, University of Bern, Sidlerstrasse 5, CH-3012 Bern, Switzerland

Received 3 March 2017; received in revised form 28 April 2017; accepted 29 April 2017
Available online 8 May 2017
Editor: Tommy Ohlsson

Abstract

Theories with extended Higgs sectors constructed in view of cosmological ramifications (gravitational wave signal, baryogenesis, dark matter) are often faced with conflicting requirements for their couplings; in particular those influencing the strength of a phase transition may be large. Large couplings compromise perturbative studies, as well as the high-temperature expansion that is invoked in dimensionally reduced lattice investigations. With the example of the inert doublet extension of the Standard Model (IDM), we show how a resummed 2-loop effective potential can be computed without a high-T expansion, and use the result to scrutinize its accuracy. With the exception of T_c, which is sensitive to contributions from heavy modes, the high-T expansion is found to perform well. 2-loop corrections weaken the transition in IDM, but they are moderate, whereby a strong transition remains an option.

1. Introduction

With the upcoming years of the LHC probing the Higgs mechanism, and the continued direct, indirect and collider searches for dark matter, together with the prospect of LISA probing gravitational wave backgrounds related to particle physics, it has become popular to search for a framework which may play a role in all contexts. Surprisingly, the Standard Model supplemented

* Corresponding author.
E-mail addresses: laine@itp.unibe.ch (M. Laine), meyer@itp.unibe.ch (M. Meyer), nardini@itp.unibe.ch (G. Nardini).

http://dx.doi.org/10.1016/j.nuclphysb.2017.04.023

by an additional scalar field, for instance in the singlet, doublet, triplet, or higher representation, cannot easily be excluded from these considerations. We focus here on the doublet case, simplified further by an additional Z(2) symmetry, a framework that is generally referred to as the Inert Doublet Model (IDM) [1–3].

The original interest in the IDM came largely from the dark matter context [4–13], which remains a viable option today (cf. e.g. refs. [14–21] and references therein). Many theoretical (cf. e.g. refs. [22–26]) and collider (cf. e.g. refs. [27–43]) constraints on the model have been considered. Furthermore, following early suggestions [44–48], a strong phase transition appears possible [49–51]. However the issue of large couplings emerges, for instance in some of the benchmarks of ref. [50] certain scalar couplings attain the magnitude $\lambda_3 \simeq 3$ in a normalization in which the Standard Model Higgs self-coupling is $\lambda_1 \simeq 0.15$.

There is a clear reason for the need for large couplings if a strong phase transition is to be present. Without any additional particles, the theory has no thermal phase transition at all (for a review, see ref. [52]). If degrees of freedom are added which are weakly coupled and massive, they can be integrated out, resulting in the same "dimensionally reduced" effective theory [53, 54] as for the Standard Model [55], and thereby with the same conclusion concerning the phase transition. To change the conclusion, we either need to add new degrees of freedom which are light around the transition point, or which come with large couplings, so that the effective couplings of the low-energy theory change by a significant amount. Light degrees of freedom could experience a transition of their own and thereby indeed influence the dynamics substantially [56, 57]; this is an interesting option but will not be considered here, given that it requires a degree of fine tuning. Thereby we are left with large couplings as the remaining avenue. It is difficult to exclude the existence of such couplings phenomenologically, given that Higgs physics does not easily avail itself to precision inspection and that constraints from fermionic processes are largely missing for the inert doublet. Large couplings do imply the presence of a nearby Landau pole and, conversely, could originate as a low-energy description of some sort of composite dynamics.

In the context of electroweak baryogenesis, a strong phase transition refers to a discontinuity $\Delta v \sim T$, where v is a gauge-fixed Higgs expectation value ($v \simeq 246$ GeV at $T = 0$), and T is the temperature [58]. In the Higgs phase, gauge boson masses are then of order $m_W \sim gv/2 \ll \pi T$, where $g \sim 2/3$ is the $\mathrm{SU_L}(2)$ gauge coupling. In this situation a high-T expansion in $m_W^2/(\pi T)^2$ works well.[1] The high-T expansion is an ingredient for instance in non-perturbative studies based on dimensional reduction (cf. e.g. refs. [59–63] and references therein). However, new degrees of freedom which get a mass through a large coupling $\lambda_3^{1/2} \sim 2$ may become heavy in the broken phase, $\lambda_3^{1/2} v \sim \pi T$. Given that the high-$T$ expansion is an asymptotic series, it is not clear whether it is numerically accurate in such a situation.

In order to test the convergence of the high-T expansion, and of the perturbative treatment in general, a sufficient loop order is needed. Here we go to 2-loop level for the effective potential. Earlier results probing the validity of the high-T expansion at 2-loop level, associated however with large vacuum masses rather than with large couplings, can be found in ref. [64]. Another related investigation, albeit restricted to an Abelian theory and without a detailed exposition of the "master" sum-integrals that appear, was presented in ref. [65].

[1] For bosonic degrees of freedom the high-T expansion also includes non-analytic terms, such as $(m_W^2)^{3/2}/(\pi T)^3$; however any sum-integral only generates a finite number of such terms, associated with Matsubara zero-mode contributions, so that they do not affect the convergence of the infinite series.

The outline of this paper is the following. After defining the IDM and the basic observables of our interest (sec. 2), we adopt a simple procedure for implementing the thermal resummations that are necessary for a consistent computation at finite temperature (sec. 3). Intricacies related to renormalization of the effective potential in the R_ξ gauge and in the presence of resummation are briefly reiterated (sec. 4). After illustrating our results numerically (sec. 5), we collect together our conclusions (sec. 6). In a number of appendices, the thermal 2-loop "master" sum-integrals used for representing the effective potential are computed, both without and with a high-T expansion (Appendix A); the 2-loop Feynman diagrams are listed in terms of these "masters" (Appendix B); and 1-loop formulae for vacuum renormalization, both as concerns the initial values of renormalization group evolution and the renormalization group evolution itself, are specified (Appendix C).

2. Model and observables

In the IDM [1–3], the Standard Model Higgs doublet, ϕ, is supplemented by an additional doublet, χ, which has the same gauge charges as ϕ but in addition displays an unbroken global Z(2) symmetry, which forbids Yukawa couplings to Standard Model fermions. The scalar potential has the form

$$\begin{aligned} V_0 = {} & \mu_1^2\,\phi^\dagger\phi + \mu_2^2\,\chi^\dagger\chi + \lambda_1\,(\phi^\dagger\phi)^2 + \lambda_2\,(\chi^\dagger\chi)^2 \\ & + \lambda_3\,\phi^\dagger\phi\,\chi^\dagger\chi + \lambda_4\,\phi^\dagger\chi\,\chi^\dagger\phi + \left\{\frac{\lambda_5}{2}\,(\phi^\dagger\chi)^2 + \text{H.c.}\right\}. \end{aligned} \tag{2.1}$$

A global phase rotation permits for us to choose λ_5 purely real and *negative*. Several extensions of the IDM have also been proposed, with additional scalars and additional gauge symmetries; many lead to fascinating phenomenology but for brevity we restrict ourselves to the simplest case here, since this is sufficient for our methodological considerations.

We are interested in the behaviour of the model at finite temperature. Simple thermodynamic characteristics of a phase transition are its critical temperature (T_c) and latent heat (L). The discontinuity of the Higgs condensate (cf. e.g. ref. [66]),

$$\frac{v_\mathrm{phys}^2}{2} \equiv Z_{\mu_1^2}\,\Delta\langle\phi^\dagger\phi\rangle\,, \tag{2.2}$$

where $Z_{\mu_1^2}$ is the renormalization factor related to the bare mass parameter μ_1^2, is a gauge-independent but scale-dependent characteristic of the transition. We choose the fixed $\overline{\mathrm{MS}}$ renormalization scale $\bar{\mu} = m_Z$ for its definition. Denoting by $f \equiv F/V$ the free energy density and by Δf its discontinuity across the transition (with $\Delta f = 0$ precisely at T_c), we can equivalently write $v_\mathrm{phys}^2/2 = \partial\Delta f/\partial\mu_1^2(m_Z)$. The importance of v_phys stems from the fact that it is strongly correlated with the rate of anomalous baryon number violation [67].

Other important characteristics of the transition are its surface tension at T_c, and the bubble nucleation rate in the whole metastability range. Determining these necessitates, however, the study of inhomogeneous configurations, which is a notoriously hard problem (cf. e.g. ref. [68]) and not addressed here. However our conclusions do support a low-energy effective theory approach, which can subsequently also be applied to this problem [69].

As a tool for computing T_c, L and v_phys we employ the effective potential. At its minima, the effective potential equals the free energy density, $f = V(v_\mathrm{min})$, up to an overall constant which drops out in $\Delta f \equiv V(v_\mathrm{min}) - V(0)$. The effective potential is defined through a shift of the neutral Higgs component by a constant, v, so that the Higgs doublets can be written as

$$\phi_{\rm R} = \frac{1}{\sqrt{2}} \begin{pmatrix} G_2 + i G_1 \\ v + h - i G_3 \end{pmatrix} , \quad \chi_{\rm R} = \frac{1}{\sqrt{2}} \begin{pmatrix} H_2 + i H_1 \\ H_0 - i H_3 \end{pmatrix} . \tag{2.3}$$

Here h represents the physical Higgs boson, and $H \equiv H_0$, $A \equiv H_3$ as well as $H_\pm = (H_1 \pm i H_2)/\sqrt{2}$ are the new scalar degrees of freedom. The Z(2) symmetry associated with χ is assumed to be unbroken, and we check this assumption *a posteriori* (see below). The meaning of v depends on the gauge choice and also on the renormalization factors Z_ϕ, Z_v (see below). Nevertheless, as has been demonstrated within the high-T expansion both for covariant [70] and R_ξ [71] gauges, gauge independent observables can be obtained from $V(v)$, in particular $\Delta f = V(v_{\rm min}) - V(0)$, which in turn fixes $T_{\rm c}$, L, and $v_{\rm phys}$ as discussed above.

3. Resummation

When we are addressing the regime $v \lesssim T$, then the masses generated by the Higgs mechanism, $m_W \sim gv/2$, are of a similar magnitude or smaller than thermal "Debye masses", $m_{\rm E2} \sim gT$. Therefore thermal masses play an important role. For the Standard Model, all thermal masses were determined in ref. [72], and a way to incorporate them at 2-loop level was worked out in ref. [73]. However, even though theoretically consistent, the procedure of ref. [73] is simple only in a setting in which a high-T expansion is valid: technically it amounts to carrying out a resummation only for Matsubara zero modes, for which it is strictly necessary. In our more general setting, in which some degrees of freedom may become heavy in the broken phase, a split-up into zero and non-zero Matsubara modes is cumbersome. Therefore, we propose to implement a *resummation for all modes*.[2] Of course, there is a price to pay for this "simplification", discussed at the end of this section and in sec. 4.4.

The set of fields for which a resummation is needed comprises the scalar fields (ϕ, χ) as well as, in covariant and R_ξ gauges, the temporal components of the gauge fields. Consider ϕ as an example. The original (imaginary-time) Lagrangian can be written as

$$\begin{aligned} L_{\rm B}(\phi_{\rm B}) &= L(\phi) + \delta L(\phi) \\ &= L(\phi) + \delta m^2_{\phi T}\, \phi^\dagger \phi + \delta L(\phi) - \delta m^2_{\phi T}\, \phi^\dagger \phi \,. \end{aligned} \tag{3.1}$$

Here $\phi_{\rm B}$ denotes a bare and $\phi \equiv \phi_{\rm R}$ a renormalized field, and δL contains the vacuum counterterms. Resummation can now be implemented by incorporating $+\delta m^2_{\phi T}\, \phi^\dagger \phi$ on par with vacuum masses in the propagators, whereas the part $\delta L(\phi) - \delta m^2_{\phi T}\, \phi^\dagger \phi$ is treated as a "counterterm". If we choose $\delta m^2_{\phi T}$ properly, i.e. as the thermal mass generated for the Matsubara zero modes, then this procedure is equivalent to the approach of ref. [73], up to corrections that are of higher order in couplings than the computation at hand.

Even though the idea just introduced is simple, the devil lies in the details, particularly in the precise choice of $\delta m^2_{\phi T}$. At high temperatures, the parametric form is $\delta m^2_{\phi T} \sim g^2 T^2 + \mathcal{O}(g^4)$. The factor T^2 originates from integrating out the non-zero Matsubara modes, so that $\delta m^2_{\phi T} \sim g^2 I_{n\neq 0}(m) + \mathcal{O}(g^4)$, where $I_{n\neq 0}(m) \equiv \sum\!\!\!\!\!\!\int_P{}' \frac{1}{P^2+m^2}$ is a tadpole integral omitting a Matsubara zero mode. Following a frequent convention, we make a choice in the following that $\delta m^2_{\phi T} \sim g^2 I(0) \equiv g^2 \sum\!\!\!\!\!\!\int_P \frac{1}{P^2}$, thereby omitting corrections of $\mathcal{O}(g^4 T^2)$ and $\mathcal{O}(g^2 m^2)$. Both approximations can be systematically lifted within the framework of dimensionally reduced theories, whereas within the approach of eq. (3.1) there is no unambiguous way to do this. We choose

[2] Analogous procedures have been pursued in other contexts, cf. e.g. refs. [74–78] and references therein.

the simple procedure because it is sufficient for addressing the main goals of our study, namely the convergence of the high-T expansion and the magnitude of 2-loop corrections. However, it should be acknowledged that this approximation is numerically questionable for the IDM: large scalar couplings imply that corrections of $\mathcal{O}(\lambda_3^2 T^2)$ can be significant, and a large mass parameter μ_2^2 implies that mass-dependent corrections of $\mathcal{O}(\lambda_3\mu_2^2)$ should be included. The omission of these corrections leads to specific problems, discussed below.

In dimensional regularization, where the space–time dimension is $D = 4 - 2\epsilon$, the sum-integral $I(0)$ contains terms of $\mathcal{O}(\epsilon)$, cf. eq. (A.17). In loop diagrams $I(0)$ can be multiplied by $1/\epsilon$, and therefore $\mathcal{O}(\epsilon)$ contributions can give finite results. The thermal masses including these pieces are listed in eqs. (4.6)–(4.9) below.

A formal crosscheck on the consistency of the resummation carried out is that the so-called "linear terms" cancel in the 2-loop result within the high-T expansion [79]. Such terms have the form $\sim g^2 I(0) I_{n=0}(m)$, where the Matsubara zero-mode part evaluates to $I_{n=0}(m) \equiv T\int_{\mathbf{p}} \frac{1}{p^2+m^2} = -\frac{mT}{4\pi}[1+\mathcal{O}(\epsilon)]$. We have analytically verified the cancellation of linear terms to all orders in ϵ within our resummation. However, as alluded to above, our simple resummation does not properly capture the infrared structure of the 2-loop potential in the IDM, in which substantial corrections of $\mathcal{O}(\lambda_3\mu_2^2)$ to the effective Higgs mass parameter can appear. This implies that the cancellation of linear terms is incomplete beyond the formal high-T limit: a remainder $\sim \lambda_3[I(\mu_2) - I(0)] I_{n=0}(m)$ is left over. In cases with $\mu_2 \gtrsim T$ such terms become visible at small v/T (cf. sec. 5.4).

4. Gauge fixing and renormalization

4.1. Gauge fixing

Perturbative computations in gauge theories require gauge fixing, even though physical observables are independent of it. For simplicity we employ the Feynman R_ξ gauge in our analysis. We also omit the hypercharge $\mathrm{U_Y}(1)$ coupling g_1, whose $\mathcal{O}(1\%)$ influence is an order of magnitude smaller than our uncertainties, and denote the weak $\mathrm{SU_L}(2)$ coupling by $g \equiv g_2$. Then the gauge fixing and Faddeev–Popov terms read

$$L_{\text{gauge fixing}} = \frac{1}{2\xi}\sum_{a=1}^{3}\Big(\partial_\mu A_\mu^a - \frac{\xi g v}{2} G_a\Big)^2 + \frac{\xi g^2 v}{4}\Big(\bar{c}_A^a\, h\, c_A^a + \epsilon^{abc}\bar{c}_A^a\, G_b\, c_A^c\Big) + \dots\,, \quad (4.1)$$

where only terms coupling to scalar degrees of freedom have been shown; G_a are Goldstone modes from eq. (2.3); and c_A^a, $\bar{c}_A^a$ are $\mathrm{SU_L}(2)$ ghost fields.

In R_ξ gauges the parameter v has two different origins: it appears as a "background field" in the gauge fixing term in eq. (4.1), and it originates from a shift of the Higgs field according to eq. (2.3). For a proper renormalization of gauge-dependent quantities, these two fields need to be kept track of and renormalized separately (cf. refs. [80,81] and references therein). The renormalization factor related to the background field is denoted by Z_v: $v_{\mathrm{B}}^2 = v^2(1+\delta Z_v)$.

4.2. Vacuum counterterms

The bare couplings are expressed as $\mu_{i\mathrm{B}}^2 = \mu_i^2\left(1+\delta Z_{\mu_i^2}\right)$, $\lambda_{i\mathrm{B}} = \lambda_i\left(1+\delta Z_{\lambda_i}\right)$, $g_{\mathrm{B}}^2 = g^2\left(1+\delta Z_{g^2}\right)$, $h_{t\mathrm{B}}^2 = h_t^2\left(1+\delta Z_{h_t^2}\right)$, where h_t is the top Yukawa coupling. Because we compute the effective potential as a function of v and because resummation treats A_0^a and A_i^a separately, we

Table 1
Tree-level masses squared in the Feynman R_ξ gauge (cf. sec. 4). The thermal mass corrections $\delta m^2_{\phi T}$, $\delta m^2_{\chi T}$, $m^2_{\rm E2}$ and $m^2_{\rm E3}$ are given in eqs. (4.6)–(4.9). By $D = 4 - 2\epsilon$ we denote the dimensionality of spacetime. The fields A_μ and C_μ correspond to the gauge groups $\mathrm{SU_L}(2)$ and SU(3), respectively, with $c_A, \bar{c}_A, c_C, \bar{c}_C$ being the Faddeev–Popov ghosts.

Field	Vacuum mass	Thermal mass	Degeneracy
h	$m_h^2 = \mu_1^2 + 3\lambda_1 v^2$	$\widetilde{m}_h^2 = m_h^2 + \delta m^2_{\phi T}$	1
G	$m_G^2 = \mu_1^2 + \lambda_1 v^2 + m_W^2$	$\widetilde{m}_G^2 = m_G^2 + \delta m^2_{\phi T}$	3
H	$m_H^2 = \mu_2^2 + \frac{1}{2}(\lambda_3 + \lambda_4 + \lambda_5) v^2$	$\widetilde{m}_H^2 = m_H^2 + \delta m^2_{\chi T}$	1
A	$m_A^2 = \mu_2^2 + \frac{1}{2}(\lambda_3 + \lambda_4 - \lambda_5) v^2$	$\widetilde{m}_A^2 = m_A^2 + \delta m^2_{\chi T}$	1
$H_\pm$	$m_{H_\pm}^2 = \mu_2^2 + \frac{1}{2}\lambda_3 v^2$	$\widetilde{m}_{H_\pm}^2 = m_{H_\pm}^2 + \delta m^2_{\chi T}$	2
A_i	$m_W^2 = \frac{1}{4} g^2 v^2$	m_W^2	$3(D-1)$
A_0	m_W^2	$\widetilde{m}_W^2 = m_W^2 + m^2_{\rm E2}$	3
$c_A, \bar{c}_A$	m_W^2	m_W^2	-6
C_i	0	0	$8(D-1)$
C_0	0	$m^2_{\rm E3}$	8
$c_C, \bar{c}_C$	0	0	-16
t	$m_t^2 = \frac{1}{2} h_t^2 v^2$	m_t^2	12

also need to renormalize certain unphysical objects, namely wave functions and the gauge fixing parameter:

$$\phi^\dagger_{\rm B}\phi_{\rm B} = \phi^\dagger\phi\left(1+\delta Z_\phi\right), \quad A^a_{\mu{\rm B}}A^a_{\nu{\rm B}} = A^a_\mu A^a_\nu\left(1+\delta Z_A\right), \quad \xi_{\rm B} = \xi\left(1+\delta Z_\xi\right). \tag{4.2}$$

The renormalized gauge parameter is set to $\xi = 1$. After the shift of the Higgs vacuum expectation value according to eq. (2.3), various counterterms are generated. For instance δL from eq. (3.1) becomes

$$\delta L(\phi) = \frac{1}{2}h\big(-\partial^2\delta Z_\phi + \delta m_h^2\big)h + \frac{1}{2}G_a\big(-\partial^2\delta Z_\phi + \delta m_G^2\big)G_a + \frac{1}{4}\delta\lambda_1 h^4 + \dots, \tag{4.3}$$

$$\delta m_h^2 = \delta\mu_1^2 + 3\,\delta\lambda_1 v^2, \quad \delta\mu_1^2 = \mu_1^2\left(\delta Z_\phi + \delta Z_{\mu_1^2}\right), \quad \delta\lambda_1 = \lambda_1\left(2\delta Z_\phi + \delta Z_{\lambda_1}\right), \tag{4.4}$$

$$\delta m_G^2 = \mu_1^2\left(\delta Z_\phi + \delta Z_{\mu_1^2}\right) + \lambda_1 v^2\left(2\delta Z_\phi + \delta Z_{\lambda_1}\right) + m_W^2\left(\delta Z_\phi + \delta Z_v + \delta Z_{g^2} + \delta Z_\xi\right). \tag{4.5}$$

Physical on-shell Green's functions, such as those listed in appendix C.3 for purposes of vacuum renormalization, are not affected by the field renormalization constants [82].

4.3. Thermal masses

With the setup introduced, the thermal mass corrections for eq. (3.1) and Table 1 read

$$\begin{aligned}\delta m^2_{\phi T} &= \left[6\lambda_1 + 2\lambda_3 + \lambda_4 + \frac{3(D-1)g_2^2}{4}\right] I(0_b) - 6h_t^2 I(0_f) \\ &= \left(\frac{3g_2^2}{16} + \frac{h_t^2}{4} + \frac{6\lambda_1 + 2\lambda_3 + \lambda_4}{12}\right) T^2 + \mathcal{O}(\epsilon\, T^2),\end{aligned} \tag{4.6}$$

$$\delta m_{\chi T}^2 = \left[6\lambda_2 + 2\lambda_3 + \lambda_4 + \frac{3(D-1)g_2^2}{4} \right] I(0_b) \tag{4.7}$$
$$= \left(\frac{3g_2^2}{16} + \frac{6\lambda_2 + 2\lambda_3 + \lambda_4}{12} \right) T^2 + \mathcal{O}(\epsilon T^2) \,,$$
$$m_{\rm E2}^2 = g_2^2(D-2)\Big[2(D-1) I(0_b) - 4 n_G I(0_f) \Big] \tag{4.8}$$
$$= \Big(1 + \frac{n_G}{3} \Big) g_2^2 T^2 + \mathcal{O}(\epsilon T^2) \,,$$
$$m_{\rm E3}^2 = g_3^2(D-2)\Big[3(D-2) I(0_b) - 4 n_G I(0_f) \Big] \tag{4.9}$$
$$= \Big(1 + \frac{n_G}{3} \Big) g_3^2 T^2 + \mathcal{O}(\epsilon T^2) \,,$$

where the function I is defined in eq. (A.8). We have adopted a notation in which 0_b and 0_f denote vanishing masses carried by bosons and fermions, respectively; and $n_G \equiv 3$ denotes the number of generations. The resulting tree-level mass spectrum is listed in Table 1.

As alluded to in the paragraphs below eq. (3.1), the leading-order "massless" resummation of eqs. (4.6)–(4.9) is not sufficient for a precise determination of $T_{\rm c}$: the effective Higgs mass parameter gets large corrections of $\mathcal{O}(\lambda_3\mu_2^2, \lambda_3^2 T^2)$ which are not properly accounted for. These corrections could be systematically included in a dimensionally reduced investigation [55,63,64], whose principal accuracy our study aims to justify.

4.4. Illustration of cancellation of divergences

The resummation introduced in eq. (3.1) modifies the divergence structure of the theory at any given loop order. Even though the changes are of higher order than the computation carried out, this leads to divergences which look worrisome at first sight. We illustrate this with the help of a single-component scalar theory,

$$V_0 = \frac{\mu_1^2 h^2}{2} \Big(1 + \delta Z_\phi + \delta Z_{\mu_1^2} \Big) + \frac{\lambda_1 h^4}{4} \Big(1 + 2\delta Z_\phi + \delta Z_{\lambda_1} \Big) \,. \tag{4.10}$$

At 1-loop level the counterterms read $\delta Z_\phi = 0$, $\delta Z_{\mu_1^2} = 3\lambda_1/(16\pi^2\epsilon)$ and $\delta Z_{\lambda_1} = 9\lambda_1/(16\pi^2\epsilon)$. The thermal mass correction is $\delta m_{\phi T}^2 = 3\lambda_1 I(0)$, and we denote $\widetilde{m}_h^2 = \mu_1^2 + 3\lambda_1 v^2 + \delta m_{\phi T}^2$.

The 1-loop effective potential is given by the function J defined in eq. (A.1): $V_1 = J(\widetilde{m}_h)$. Writing $V_1 = \sum_{n=-1}^{\infty} V_1^{(n)} \epsilon^n$, let us consider the divergent part, given by eq. (A.4), *viz.*

$$\frac{V_1^{(-1)}}{\epsilon} = -\frac{\widetilde{m}_h^4}{64\pi^2\epsilon}$$
$$= -\frac{6\lambda_1\mu_1^2 v^2 + 9\lambda_1^2 v^4 + 2\delta m_{\phi T}^2 [\mu_1^2 + 3\lambda_1 v^2]}{64\pi^2\epsilon} + (v\text{-independent}) \,. \tag{4.11}$$

The T-independent divergences $\propto \mu_1^2 v^2, v^4$ are cancelled by the counterterms in eq. (4.10). In contrast, the T-dependent divergence $\propto \delta m_{\phi T}^2$ is only cancelled by a part of V_2, as we show below. This is the peculiarity related to thermal divergences within the resummation we have adopted: whereas vacuum divergences are cancelled by counterterms originating from *lower-order* diagrams (V_0), thermal divergences are cancelled by the appearance of $\delta m_{\phi T}^2$ within *higher-order* contributions (V_2).

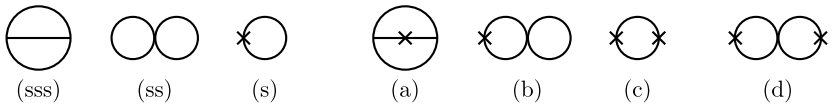

Fig. 1. Topologies of the diagrams discussed in sec. 4.4. The cross denotes a contribution from counterterms including the "thermal mass", $-\delta m^2_{\phi T}\,\phi^\dagger\phi$ in eq. (3.1), which is counted on par with a vertex in the resummed computation. Therefore, the graphs (sss), (ss) and (s) are of "2-loop order"; the graphs (a), (b) and (c) of "3-loop order"; and the graph (d) of "4-loop order".

There are three diagrams contributing to V_2 (cf. Fig. 1): a "sunset" diagram containing three propagators, denoted by (sss); a "figure-8" diagram containing two propagators, denoted by (ss); and a counterterm diagram containing one propagator, denoted by (s). Making use of the notation of Appendix A, the expressions read

$$V_2 = (\mathrm{sss}) + (\mathrm{ss}) + (\mathrm{s})\,, \tag{4.12}$$

$$(\mathrm{sss}) = -3v^2\lambda_1^2\, H(\widetilde{m}_h, \widetilde{m}_h, \widetilde{m}_h)\,, \tag{4.13}$$

$$(\mathrm{ss}) = \frac{3\lambda_1 I(\widetilde{m}_h) I(\widetilde{m}_h)}{4}\,, \tag{4.14}$$

$$(\mathrm{s}) = \frac{\mu_1^2\,\delta Z_{\mu_1^2} + 3\lambda_1 v^2\,\delta Z_{\lambda_1} - \delta m^2_{\phi T}}{2}\, I(\widetilde{m}_h)\,. \tag{4.15}$$

The sum of eqs. (4.13)–(4.15) contains divergences of orders $1/\epsilon^2$ and $1/\epsilon$, cf. eqs. (A.11), (A.33) and (A.34). Writing $V_2 = \sum_{n=-2}^{\infty} V_2^{(n)}\epsilon^n$, the $1/\epsilon^2$ divergences sum up to

$$\frac{V_2^{(-2)}}{\epsilon^2} = \frac{3\lambda_1[\delta m^2_{\phi T} + \mu_1^2 + 3\lambda_1 v^2][\delta m^2_{\phi T} - \mu_1^2 - 9\lambda_1 v^2]}{4(4\pi)^4\epsilon^2}\,. \tag{4.16}$$

The T-independent parts $\propto \mu_1^2 v^2, v^4$ can be taken care of by 2-loop contributions to δZ_ϕ, $\delta Z_{\mu_1^2}$ and δZ_{λ_1} in eq. (4.10). However, a T and v-dependent part $\sim \lambda_1^2 v^2 \delta m^2_{\phi T}/\epsilon^2$ remains. This is only cancelled by diagrams in which the insertion $\delta m^2_{\phi T}$ appears inside 2-loop topologies, which are counted on par with diagrams of 3-loop order (diagrams (a) and (b) in Fig. 1). There is also a T-dependent but v-independent term $\sim \lambda_1 \delta m^4_{\phi T}/\epsilon^2$ which is cancelled by 2-loop topologies containing two insertions of $\delta m^2_{\phi T}$, a contribution which is counted on par with diagrams of 4-loop order (diagram (d) in Fig. 1).

As far as the divergences of order $1/\epsilon$ go, the term proportional to $\delta m^2_{\phi T}$ in eq. (4.15) exactly cancels against the 1-loop contribution in eq. (4.11), apart from a v-independent divergence $\sim \delta m^4_{\phi T}/\epsilon$. This gets cancelled by a 1-loop topology dressed by two appearances of $\delta m^2_{\phi T}$, which is counted on par with diagrams of 3-loop order (diagram (c) in Fig. 1).

A non-trivial cancellation is observed by considering $1/\epsilon$-divergences proportional to the non-analytic structure $-\widetilde{m}_h^2/(4\pi)^2 \ln\bigl(\bar{\mu}^2/\widetilde{m}_h^2\bigr) + I_T^{(0)}(\widetilde{m}_h)$, originating from $I^2(\widetilde{m}_h)$ and $H(\widetilde{m}_h, \widetilde{m}_h, \widetilde{m}_h)$ as shown by eqs. (A.12) and (A.34), respectively. We find that vacuum parts $\propto \lambda_1\mu_1^2, \lambda_1^2 v^2$ cancel from the coefficient of this divergence, as is required by renormalizability. The remainder reads

$$\left.\frac{V_2^{(-1)}}{\epsilon}\right|_{\text{non-analytic}} = -\frac{3\lambda_1\delta m^2_{\phi T}}{2(4\pi)^2\epsilon}\left[-\frac{\widetilde{m}_h^2}{(4\pi)^2}\ln\left(\frac{\bar{\mu}^2}{\widetilde{m}_h^2}\right) + I_T^{(0)}(\widetilde{m}_h)\right]. \tag{4.17}$$

Again this is only cancelled by diagrams in which the insertion $\delta m_{\phi T}^2$ appears inside 2-loop topologies, which are counted on par with 3-loop graphs (diagrams (a) and (b) in Fig. 1).

To summarize, one price we pay for the resummation introduced in sec. 3 is that ultraviolet divergences do not cancel order by order in our power counting, in which the last term of eq. (3.1) is treated as an insertion. Instead thermal divergences cancel once all insertions contributing to a given order in couplings have been accounted for. This "drawback" is compensated for by the fact that infrared sensitive terms get resummed to all orders.

5. Results

5.1. Diagrams

At tree and 1-loop levels the effective potential follows from the Lagrangian in eq. (2.1) and from 1-loop contributions in terms of the sum-integral J defined in appendix A.1. With masses and degeneracies as listed in Table 1, we get

$$\begin{aligned} V_0 + V_1 = {} & \frac{\mu_1^2 v^2}{2} + \frac{\lambda_1 v^4}{4} + \frac{\delta\mu_1^2 v^2}{2} + \frac{\delta\lambda_1 v^4}{4} \\ & + J(\widetilde{m}_h) + 3J(\widetilde{m}_G) + J(\widetilde{m}_H) + J(\widetilde{m}_A) + 2J(\widetilde{m}_{H_\pm}) \\ & + 3\Big[(D-3)J(m_W) + J(\widetilde{m}_W)\Big] + 8\Big[(D-3)J(0_b) + J(m_{\rm E3})\Big] \\ & - 12J(m_t) - (30n_G - 12)J(0_f)\,, \end{aligned} \tag{5.1}$$

where the counterterms are from eq. (4.4). The 2-loop diagrams are given in Appendix B.

5.2. Cancellation of divergences

The cancellation of divergences through vacuum counterterms offers for a useful crosscheck of the computation. As illustrated in sec. 4.4, the cancellation is non-trivial and incomplete in the presence of the thermal resummation introduced in eq. (3.1). We briefly summarize here the cancellations that can be observed.

First of all, vacuum (i.e. temperature independent) divergences are cancelled by counterterms of a *lower* loop order. Parametrically, the tree-level potential V_0 is of order m^4/g^2. The 1-loop contribution V_1 is of order m^4 and contains divergences. These are cancelled by tree-level counterterms $\delta Z \sim g^2$, which modify V_0 by effects of $\sim V_0\,\delta Z \sim m^4$. Similarly, V_2 is of order $g^2 m^4$ and contains divergences. These are cancelled by contributions of $\sim g^4$ to δZ appearing in $V_0 \sim m^4/g^2$, and by 1-loop effects containing the counterterms, likewise of order $V_1 \delta Z \sim g^2 m^4$.

In contrast, thermal divergences are cancelled by *higher-order* effects. When the thermal masses of Table 1 are used within the 1-loop expression, cf. eq. (5.1), then the divergent part of the function J, cf. eq. (A.4), leads to temperature-dependent divergences. Writing $V_1 = V_1^{(-1)}/\epsilon + V_1^{(0)} + \ldots$ and denoting the thermal part by $V_{1,T}^{(-1)}$, we get

$$\begin{aligned} \frac{V_{1,T}^{(-1)}}{\epsilon} = {} & -\frac{\delta m_{\phi T}^2\,(m_h^2 + 3m_G^2) + \delta m_{\chi T}^2\,(m_H^2 + m_A^2 + 2m_{H_\pm}^2) + 3m_{\rm E2}^2 m_W^2}{2(4\pi)^2\epsilon} \\ & + (v\text{-independent})\,. \end{aligned} \tag{5.2}$$

Recalling the divergent part of the function I as given in eq. (A.11), eq. (5.2) is cancelled by the parts of V_2 given in eqs. (B.3) and (B.11) that contain the thermal counterterms:

Table 2
The benchmark scenarios from ref. [50]. The values of $(\lambda_3+\lambda_4+\lambda_5)/2$ and λ_2 refer to the renormalization scale $\bar{\mu}=m_Z$. The smallness of $(\lambda_3+\lambda_4+\lambda_5)/2$ was justified with dark matter relic density considerations, and that of λ_2 with constraints from dark matter self-interactions.

Scenario	m_H/GeV	m_A/GeV	$m_{H_\pm}$/GeV	$(\lambda_3+\lambda_4+\lambda_5)(m_Z)/2$	$\lambda_2(m_Z)$
BM1	66	300	300	1.07×10^{-2}	0.01
BM2	200	400	400	1.00×10^{-2}	0.01
BM3	5	265	265	-0.60×10^{-2}	0.01

$$\text{(s)}+\text{(v)}=-\frac{1}{2}\Bigg\{\delta m^2_{\phi T}\Big[I(\widetilde{m}_h)+3I(\widetilde{m}_G)\Big]+\delta m^2_{\chi T}\Big[I(\widetilde{m}_H)+I(\widetilde{m}_A)+2I(\widetilde{m}_{H_\pm})\Big] + 3m^2_{\text{E2}}I(\widetilde{m}_W)\Bigg\}\,. \tag{5.3}$$

There is a v-independent remainder $\propto \delta m^4_{\phi T}/\epsilon$ left over which is fully cancelled only once the "3-loop" diagram (c) in Fig. 1 is included, as discussed in sec. 4.4.

A stringent test is given by the cancellation of non-analytic divergences, of the type in eq. (4.17). We find that divergences proportional to the functions $I^{(0)}_T(\underline{m_W})$, $I^{(0)}_T(\underline{\widetilde{m}_W})$, $I^{(0)}_T(\widetilde{m}_h)$, $I^{(0)}_T(\widetilde{m}_G)$, $I^{(0)}_T(\widetilde{m}_H)$, $I^{(0)}_T(\widetilde{m}_A)$, $I^{(0)}_T(\widetilde{m}_{H_\pm})$, $I^{(0)}_T(m_W)$ and $I^{(0)}_T(\widetilde{m}_W)$ do cancel, apart from terms proportional to thermal masses, which are cancelled by higher-order contributions as discussed in sec. 4.4.

In our practical procedure, we let the divergences be cancelled by the vacuum counterterms to the extent that this happens. The remaining divergences, which are proportional to thermal masses and thereby formally of higher order, are removed by hand. Furthermore, because divergences proportional to thermal masses do cancel at higher order, we do *not* expand the thermal masses in ϵ, but remove these divergences as a whole. This implies, for instance, that the finite part of the 1-loop contribution in eq. (5.1) becomes

$$\begin{aligned}V^{(0)}_1 &= J^{(0)}(\widetilde{m}_h)+3J^{(0)}(\widetilde{m}_G)+J^{(0)}(\widetilde{m}_H)+J^{(0)}(\widetilde{m}_A)+2J^{(0)}(\widetilde{m}_{H_\pm})\\ &\quad+3\big[J^{(0)}(m_W)-2J^{(-1)}(m_W)+J^{(0)}(\widetilde{m}_W)\big]\\ &\quad+8\big[J^{(0)}(0_b)-2J^{(-1)}(0_b)+J^{(0)}(m_{\text{E3}})\big]\\ &\quad-12J^{(0)}(m_t)-(30n_G-12)J^{(0)}(0_f)\,,\end{aligned} \tag{5.4}$$

where the functions $J^{(-1)}$ and $J^{(0)}$ are from eqs. (A.4) and (A.5), respectively. Similarly, the 2-loop potential $V^{(2)}$ contains contributions of the types $I^{(0)}I^{(0)}$, $I^{(-1)}I^{(1)}$, $H^{(0)}$ and, from coefficients containing $D=4-2\epsilon$, $I^{(-1)}I^{(0)}$ and $H^{(-1)}$.

5.3. Fixing the couplings

For numerical evaluations we focus on three benchmark points, introduced in ref. [50]. As it turns out, this is sufficient for addressing generic issues concerning the high-T expansion and the convergence of the perturbative expansion. The physical parameters associated with these benchmarks are listed in Table 2.

A common feature of all the benchmark points is that the mass splittings in the inert sector are larger than would "naturally" be expected from electroweak symmetry breaking, specifically $m_A-m_H\gg m_Z$ and $m_{H_\pm}-m_H\gg m_Z$. This assumption necessitates some of the inert scalar

Table 3
Values of $\overline{\rm MS}$ couplings at the scale $\bar{\mu} = m_Z$, obtained as explained in appendix C.4. Here "2-loop" signals that a subset of 2-loop corrections was included in μ_1^2 and λ_1. For the thermal analysis the values are treated as fixed input, so more digits have been given than are physically accurate.

	BM1		BM2		BM3	
	1-loop	"2-loop"	1-loop	"2-loop"	1-loop	"2-loop"
$\mu_1^2(m_Z)/\mathrm{GeV}^2$	−6669	−6568	−8463	−8127	−7392	−7251
$\mu_2^2(m_Z)/\mathrm{GeV}^2$	842	842	36620	36620	−1243	−1243
$\lambda_1(m_Z)$	0.0670	0.0634	0.0671	0.0579	0.1021	0.0979
$\lambda_2(m_Z)$	0.010	0.010	0.010	0.010	0.010	0.010
$\lambda_3(m_Z)$	2.757	2.757	2.618	2.618	2.243	2.243
$\lambda_4(m_Z)$	−1.368	−1.368	−1.299	−1.299	−1.127	−1.127
$\lambda_5(m_Z)$	−1.368	−1.368	−1.299	−1.299	−1.127	−1.127
$g_2^2(m_Z)$	0.425	0.425	0.425	0.425	0.425	0.425
$g_3^2(m_Z)$	1.489	1.489	1.489	1.489	1.489	1.489
$h_t^2(m_Z)$	0.971	0.971	0.973	0.973	0.969	0.969

self-couplings to be large. In fact, the couplings are so large that 1-loop corrections to physical parameters, such as pole masses, are of order unity. The ingredient from vacuum renormalization that is relevant for our study is the determination of the values of all $\overline{\rm MS}$ parameters at some reference scale, chosen as $\bar{\mu} = m_Z$ in accordance with ref. [50]. The procedure that we have adopted for estimating these values is to employ a "self-consistent" prescription in order to resum a subset of higher-order corrections and thereby to delimit the magnitude of loop effects; details are deferred to appendix C.4.[3] The resulting couplings are listed in Table 3. For the remainder of this study, we can forget about vacuum renormalization and simply use the values in Table 3 as input. We have checked that variations of the renormalization prescription, which lead to $\mathcal{O}(20\%)$ variations of μ_1^2 and λ_1 for BM2, nevertheless leave our physics conclusions concerning thermal effects qualitatively intact.

An important first observation from Table 3 is that the Higgs self-coupling λ_1 can be smaller than in the Standard Model, $\lambda_1(m_Z) \simeq 0.07 \ll 0.15$. A small quartic coupling favours a strong phase transition. However, for thermal considerations, the renormalization scale permitting to avoid large logarithms differs from that used for vacuum renormalization. Specifically, thermal fluctuations introduce logarithms of the type $\ln(\bar{\mu}/(\pi T))$ [55]. Therefore at finite temperature we use

$$\bar{\mu} = \alpha \bar{\mu}_T \,, \quad \bar{\mu}_T \equiv \pi T \,, \quad \alpha \in (0.5, 2.0) \,. \tag{5.5}$$

The couplings are run between $\bar{\mu} = m_Z$ and $\bar{\mu} = \alpha \bar{\mu}_T$ according to 1-loop renormalization group equations as specified in appendix C.5. We believe that uncertainties from higher-order corrections to the running are of secondary importance for the qualitative issues that we are addressing, particularly the convergence of the high-T expansion.

[3] To summarize briefly, the Higgs sector parameters μ_1^2, λ_1 are evaluated *à la* Coleman–Weinberg; the other couplings are evaluated iteratively such that the same values appear on both sides of the equation.

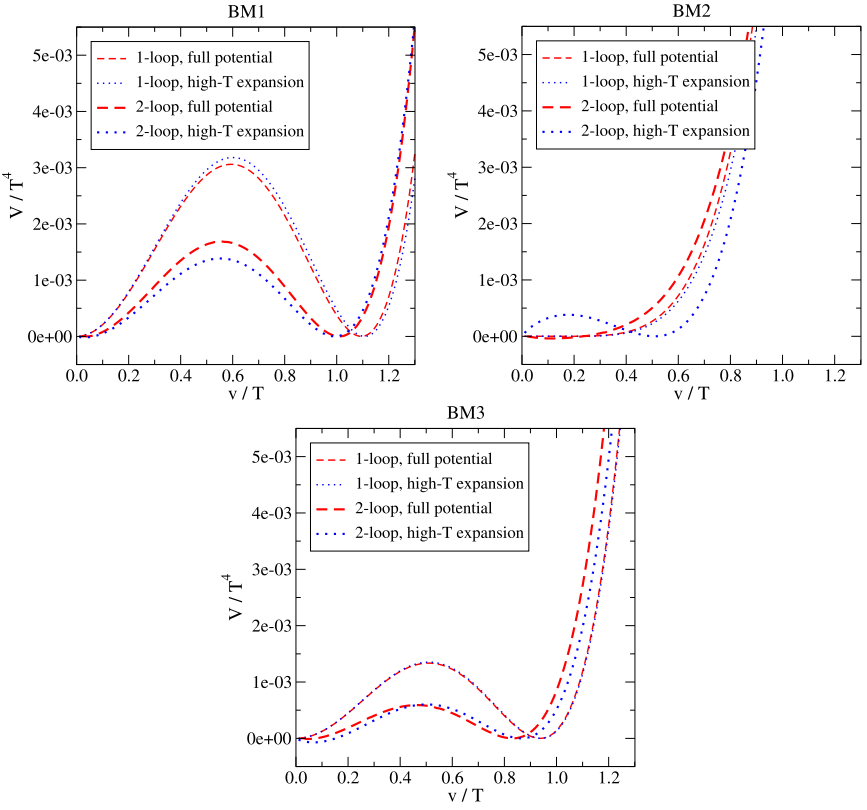

Fig. 2. Resummed 1-loop and 2-loop effective potentials, both with and without the high-T expansion, close to the respective critical temperatures, for the various benchmark points listed in Table 2. We stress that, as elaborated upon in secs. 4 and 5.2, the effective potential is gauge dependent and in the presence of resummation contains uncancelled divergences at any finite loop order, with "loop order" defined in the sense of Fig. 1; hence the plots are meant for illustration only. The gauge-independent results that can be derived from the effective potential are given in Table 4.

5.4. Numerical evaluation

We have evaluated the 1-loop and 2-loop effective potentials both in a closed form utilizing the high-T expansion, and numerically without resorting to it.

As discussed above, the computation is theoretically consistent only in stable phases: the "symmetric phase" at high temperatures and the "Higgs phase" at low temperatures. Outside of these phases the results are gauge dependent. In addition the results contain uncancelled ultraviolet divergences at any finite loop order as discussed in secs. 4.4 and 5.2. Once the ultraviolet divergences are removed by hand, an uncancelled $\bar{\mu}$-dependence is left over. Furthermore, some masses may become tachyonic; we replace the masses squared by their absolute values in such cases. However, these ambiguities are numerically benign in comparison with the "physical" uncertainty associated with scale dependence, which is formally of higher order but in practice substantial, given the large values of some of the mass parameters and couplings. This uncertainty is estimated through the scale variation in eq. (5.5).

We assume in this paper that the Z(2) symmetry related to the Inert Doublet χ is unbroken. In order to verify the validity of this assumption, the effective mass squared of the χ

Table 4
Results for the physical quantities defined in sec. 2, as well as for the gauge dependent $v_{\rm min}$ evaluated in Feynman R_ξ gauge, for the benchmark scenarios listed in Table 2. The uncertainties were obtained through the scale variation in eq. (5.5). We note that the scale uncertainties, which reflect the size of higher-order corrections from large scalar couplings, completely dominate over ambiguities related to gauge dependence, whose size is indicated by the difference between $v_{\rm phys}$ and $v_{\rm min}$.

Full effective potential

	$T_{\rm c}/{\rm GeV}$		$L/T_{\rm c}^4$		$v_{\rm phys}/T_{\rm c}$		$v_{\rm min}/T_{\rm c}$	
	1-loop	2-loop	1-loop	2-loop	1-loop	2-loop	1-loop	2-loop
BM1	139(14)	155(21)	0.44(1)	0.34(1)	1.14(12)	0.98(4)	1.15(12)	0.98(3)
BM2	159(13)	181(22)	0.07(7)	0.03(3)	0.39(28)	0.16(16)	0.39(28)	0.17(17)
BM3	138(8)	167(19)	0.35(3)	0.20(1)	0.96(10)	0.84(6)	0.98(10)	0.81(2)

High-T expansion

	$T_{\rm c}/{\rm GeV}$		$L/T_{\rm c}^4$		$v_{\rm phys}/T_{\rm c}$		$v_{\rm min}/T_{\rm c}$	
	1-loop	2-loop	1-loop	2-loop	1-loop	2-loop	1-loop	2-loop
BM1	140(14)	124(8)	0.45(1)	0.49(22)	1.15(13)	1.04(31)	1.16(13)	1.05(32)
BM2	159(14)	140(9)	0.08(8)	0.16(8)	0.42(30)	0.60(19)	0.42(30)	0.60(19)
BM3	138(8)	125(3)	0.35(3)	0.37(16)	0.97(10)	0.89(23)	0.98(10)	0.91(23)

field, $\mu_2^2 + \delta m_{\chi T}^2$ in the notation of Table 1, is evaluated at the critical temperature. We find $\mu_2^2 + \delta m_{\chi T}^2 \gtrsim (0.6T)^2$ in all cases, justifying the assumption *a posteriori*, given that $0.6T \sim gT$ is parametrically a "heavy" scale, similar to $m_{\rm E2}$.

In Fig. 2, the 1-loop and 2-loop effective potentials are plotted at the corresponding critical temperatures, both with and without a high-T expansion. We note that the 2-loop corrections are substantial but in general they do not modify the 1-loop predictions qualitatively. For BM1 and BM3 they weaken the transition moderately, and for BM2 they remove the transition altogether for $\bar{\mu} \gtrsim \bar{\mu}_T$ (in contrast they appear to strengthen the transition for BM2 within the high-T expansion, however those results are unreliable because of the large value of μ_2^2). With the exception of BM2, the high-T expansion is seen to work very well. However, the value of the critical temperature does change substantially through the high-T expansion; this is easily understood and is elaborated upon in sec. 6.

For BM2, in which case we find a very weak transition, the problems mentioned at the end of sec. 3, associated on one hand with the breakdown of the high-T expansion for heavy inert modes (cf. Table 3), and on the other with infrared sensitive terms not captured by our simple thermal resummation, become visible as "linear terms" at small v/T. We do not elaborate on these any further, given that the transition is too weak to be of physical interest.

Physical (gauge independent) results for the quantities $T_{\rm c}$, L and $v_{\rm phys}$, defined in sec. 2, are collected in Table 4. The errors originate from a variation of $\bar{\mu}$ in the range $(0.5...2.0)\,\pi T$, cf. eq. (5.5). These results confirm the heuristic impressions visible in Fig. 2. At least for BM1, the transition could be marginally strong enough to support electroweak baryogenesis.

6. Conclusions

In this paper we have developed the general technology for evaluating the full 2-loop thermal effective potential for the Higgs field, without resorting to a high-temperature expansion. The

technology has been applied to the Inert Doublet Model (IDM), incorporating thermal resummation in a particularly simple way.

Even though we did not dwell on this in the text, the largest technical effort of our work went into the derivation of the formulae given in Appendices A and B, and into their numerical evaluation, which poses a challenge of its own (some remarks can be found in a paragraph below eq. (A.45)). The results of Appendix A are model-independent, and can be applied to any extension of the Standard Model.

A word of caution is in order on the simple resummation that we adopted (sec. 3). As explained at the end of sec. 3 and in sec. 5.4, the resummation is not suitable for a precise treatment of infrared effects; at the same time, as explained in secs. 4.4 and 5.2, it is also problematic in the ultraviolet, introducing spurious divergences which are only cancelled by higher-order diagrams. We therefore do not endorse its use for *practical computations* aiming at physical precision; for us it was just a simple tool permitting to compare two different computations (a full 2-loop analysis and its high-T expansion). As explained below, our final conclusion concerning the high-T expansion suggests the availability of *other tools* for addressing physical observables with good precision.

Applying the formalism to the IDM as an example, our main finding is that the high-T expansion works well for describing the strength of the phase transition, despite the fact that some degrees of freedom become heavy in the Higgs phase (cf. Fig. 2 and Table 4). This is a welcome observation, given that it opens the avenue for dimensionally reduced lattice investigations, necessary for cases in which a good precision is needed and/or properties associated with inhomogeneous configurations are of interest. This concerns for instance the surface tension [59,60], the bubble nucleation rate [69], and the sphaleron rate [67].

Based on the benchmark points considered, as well as on a parameter scan at 1-loop level, we find that in general the IDM transition is at most moderately strong, as long as the χ-field does not become so light that it would experience a transition of its own. In other models, possessing a stronger transition, the high-T expansion could fail. At the same time, we would expect smaller 2-loop corrections in those cases, given that the infrared sensitive expansion parameter is $\sim g^2T/(\pi m_W) \sim 2gT/(\pi v)$.

There is one observable for which the high-T expansion does *not* work well: the critical temperature T_c (cf. the 2-loop results in Table 4). This should not come as a surprise: some of the inert scalars *are* heavy and/or strongly coupled, and should not be treated with the high-T expansion nor with the leading-order resummation of sec. 3. Even though they have little effect on the phase transition, they "renormalize" the effective Higgs mass parameter by a large amount. Within a dimensionally reduced investigation [53,54], these effects can be incorporated without a high-T expansion [64] and including higher orders in large couplings [55], so a good precision can be expected also for T_c. We believe that a detour through the dimensionally reduced description, with effects of $\mathcal{O}(\lambda_3\mu_2^2)$ and $\mathcal{O}(\lambda_3^2T^2)$ included in thermal masses, should be chosen even in purely perturbative studies, if numerical precision at or below the 10% level is needed.

Turning finally to cosmology, our study supports previous suggestions according to which the IDM can incorporate a phase transition marginally strong enough for baryogenesis, at least for the benchmark point BM1 (cf. Table 4). The 2-loop corrections weaken the transition somewhat, but in many cases they also reduce the scale uncertainties of L, $v_{\rm phys}$ and $v_{\rm min}$ (cf. the panel "full effective potential" in Table 4). However the problem of obtaining sufficient CP violation is not alleviated by the IDM Higgs sector which contains no new physical phases. As an example of a work-around, it has been suggested that CP violation in the interactions responsible for neutrino masses could play a role for baryogenesis (cf. e.g. ref. [83]).

Acknowledgements

This work was supported by the Swiss National Science Foundation (SNF) under grant 200020-168988, and by the Munich Institute for Astro- and Particle Physics (MIAPP) of the DFG cluster of excellence "Origin and Structure of the Universe".

Appendix A. Thermal master sum-integrals

We list here the expressions for the sum-integrals that are needed for evaluating the 2-loop effective potential. The results are divergent for $\epsilon \to 0$. For the 1-loop structures the divergences are proportional to $1/\epsilon$; the 2-loop result contains squares of 1-loop structures, so that the 1-loop structures need to be evaluated up to terms of $\mathcal{O}(\epsilon)$. For genuine 2-loop structures, the terms that need to be tracked are of $\mathcal{O}(1/\epsilon^2)$, $\mathcal{O}(1/\epsilon)$, and $\mathcal{O}(1)$.

The master sum-integrals contain both vacuum (i.e. temperature independent) and thermal parts. In the following, the thermal corrections are given both in an exact form suitable for numerical evaluation, and analytically in a high-T expansion. In the latter case, the leading contribution is of $\mathcal{O}(T^4)$, and we list terms up to $\mathcal{O}(m^4, g^2m^2T^2)$, where m^2 denotes a generic mass squared and g^2 a generic coupling constant. This is consistent with a power counting $m^2 \lesssim g^2T^2$ which can be used for justifying the high-T expansion. Some of the master structures are always multiplied by $\sim g^2m^2$, in which case high-T expansions are given up to $\mathcal{O}(T^2)$.

Thermal corrections depend on whether the particle in question is a boson or a fermion. In order to compactify the expressions, we employ an implicit notation in which the statistics is identified through the mass carried by the particle. The distribution function is denoted generically by n, and if the argument is "bosonic", it is to be interpreted as the Bose distribution, $n(\omega) \to n_{\rm B}(\omega) \equiv 1/(e^{\omega/T} - 1)$. In contrast, with a "fermionic" argument, minus the Fermi distribution is to be understood, $n(\omega) \to -n_{\rm F}(\omega) \equiv -1/(e^{\omega/T} + 1)$. A vanishing bosonic mass is denoted by 0_b and a fermionic one by 0_f.

A.1. Function $J(m)$

The master sum-integral appearing in the 1-loop result is denoted by

$$J(m) \equiv \frac{1}{2}\sum\!\!\!\!\!\!\int_P \ln\bigl(P^2+m^2\bigr) = \frac{m^2A(m)}{D} - \frac{1}{D-1}\int_{\mathbf{p}} \frac{p^2 n(\omega)}{\omega}\,, \tag{A.1}$$

where $P = (\omega_n, \mathbf{p})$; ω_n denote Matsubara frequencies; $p \equiv |\mathbf{p}|$; the vacuum function A is given in eq. (C.1); $D = 4-2\epsilon$; $\omega_i \equiv \sqrt{p^2+m_i^2}$; and we made use of partial integrations and properties of dimensional regularization. We write

$$J(m) = \frac{1}{\epsilon}\,J^{(-1)}(m) + J^{(0)}(m) + \mathcal{O}(\epsilon)\,. \tag{A.2}$$

Suppressing an overall $\mu^{-2\epsilon}$, where μ is a scale parameter related to dimensional regularization, and denoting

$$\ln\bar{\mu}^2 \equiv \ln\mu^2 + \ln(4\pi) - \gamma_{\rm E}\,, \tag{A.3}$$

the expressions for the functions in eq. (A.2) read

$$J^{(-1)}(m) = -\frac{m^4}{4(4\pi)^2}\,, \tag{A.4}$$

$$J^{(0)}(m) = -\frac{m^4}{4(4\pi)^2}\biggl(\ln\frac{\bar{\mu}^2}{m^2} + \frac{3}{2}\biggr) - \frac{I_T^{(0)}(\underline{m})}{3}\,, \tag{A.5}$$

where $I_T^{(0)}(\underline{m})$ is given in eq. (A.24). In the high-T limit, the expressions depend on whether bosonic or fermionic particles are considered. Expanding up to $\mathcal{O}(m^4)$, the bosonic contributions read

$$J^{(0)}(m_b) = -\frac{\pi^2T^4}{90} + \frac{m_b^2T^2}{24} - \frac{m_b^3T}{12\pi} - \frac{m_b^4}{2(4\pi)^2}\ln\biggl(\frac{\bar{\mu}e^{\gamma_{\rm E}}}{4\pi T}\biggr) + \mathcal{O}\biggl(\frac{m_b^6}{\pi^4T^2}\biggr)\,, \tag{A.6}$$

whereas the fermionic expression is

$$J^{(0)}(m_f) = \frac{7}{8}\frac{\pi^2T^4}{90} - \frac{m_f^2T^2}{48} - \frac{m_f^4}{2(4\pi)^2}\ln\biggl(\frac{\bar{\mu}e^{\gamma_{\rm E}}}{\pi T}\biggr) + \mathcal{O}\biggl(\frac{m_f^6}{\pi^4T^2}\biggr)\,. \tag{A.7}$$

A.2. Function $I(m)$

The basic 1-loop structure appearing within the 2-loop result is denoted by

$$I(m) \equiv \sum\!\!\!\!\!\!\int_P \frac{1}{P^2+m^2} = A(m) + \int_{\mathbf{p}}\frac{n(\omega)}{\omega}\,, \tag{A.8}$$

where the vacuum part A is from eq. (C.1). We write

$$I(m) = \frac{1}{\epsilon}\,I^{(-1)}(m) + I^{(0)}(m) + \epsilon\,I^{(1)}(m) + \mathcal{O}(\epsilon^2)\,, \tag{A.9}$$

and subsequently separate each contribution into a vacuum and thermal part,

$$I^{(n)}(m) = I_0^{(n)}(m) + I_T^{(n)}(m)\,. \tag{A.10}$$

Suppressing an overall $\mu^{-2\epsilon}$, the expressions for the functions in eq. (A.9) read

$$I^{(-1)}(m) = -\frac{m^2}{(4\pi)^2}\,, \tag{A.11}$$

$$I^{(0)}(m) = -\frac{m^2}{(4\pi)^2}\biggl(\ln\frac{\bar{\mu}^2}{m^2} + 1\biggr) + I_T^{(0)}(m)\,, \tag{A.12}$$

$$I_T^{(0)}(m) = \int_0^\infty \frac{{\rm d}p\,p^2\,n(\omega)}{2\pi^2\omega}\,, \tag{A.13}$$

$$I^{(1)}(m) = -\frac{m^2}{(4\pi)^2}\biggl(\frac{1}{2}\ln^2\frac{\bar{\mu}^2}{m^2} + \ln\frac{\bar{\mu}^2}{m^2} + 1 + \frac{\pi^2}{12}\biggr) + I_T^{(1)}(m)\,, \tag{A.14}$$

$$I_T^{(1)}(m) = \int_0^\infty \frac{{\rm d}p\,p^2\,(\ln\frac{\bar{\mu}^2}{4p^2} + 2)n(\omega)}{2\pi^2\omega}\,. \tag{A.15}$$

These functions are related through $I^{(n)}(m) = \bar{\mu}^2\partial I^{(n+1)}(m)/\partial\bar{\mu}^2$. In the high-$T$ limit, the bosonic contributions read

$$I^{(0)}(m_b) = \frac{T^2}{12} - \frac{m_b T}{4\pi} - \frac{2m_b^2}{(4\pi)^2}\ln\biggl(\frac{\bar{\mu}e^{\gamma_{\rm E}}}{4\pi T}\biggr) + \mathcal{O}\biggl(\frac{m_b^4}{\pi^4 T^2}\biggr)\,, \tag{A.16}$$

$$\begin{aligned} I^{(1)}(m_b) = {} & \frac{T^2}{6}\biggl[\ln\biggl(\frac{\bar{\mu}e^{\gamma_{\rm E}}}{2T}\biggr) - \frac{\zeta'(2)}{\zeta(2)}\biggr] - \frac{m_b T}{2\pi}\biggl[\ln\biggl(\frac{\bar{\mu}}{2m_b}\biggr) + 1\biggr] \\ & - \frac{2m_b^2}{(4\pi)^2}\biggl[\ln^2\biggl(\frac{\bar{\mu}e^{\gamma_{\rm E}}}{4\pi T}\biggr) - \gamma_{\rm E}^2 - 2\gamma_1 + \frac{\pi^2}{8}\biggr] + \mathcal{O}\biggl(\frac{m_b^4}{\pi^4 T^2}\biggr)\,, \end{aligned} \tag{A.17}$$

where the Stieltjes constant γ_1 is defined through $\zeta(s) = 1/(s-1) + \sum_{n=0}^{\infty}\gamma_n(-1)^n(s-1)^n/n!$. The corresponding fermionic expressions are

$$I^{(0)}(m_f) = -\frac{T^2}{24} - \frac{2m_f^2}{(4\pi)^2}\ln\biggl(\frac{\bar{\mu}e^{\gamma_{\rm E}}}{\pi T}\biggr) + \mathcal{O}\biggl(\frac{m_f^4}{\pi^4 T^2}\biggr)\,, \tag{A.18}$$

$$\begin{aligned} I^{(1)}(m_f) = {} & -\frac{T^2}{12}\biggl[\ln\biggl(\frac{\bar{\mu}e^{\gamma_{\rm E}}}{4T}\biggr) - \frac{\zeta'(2)}{\zeta(2)}\biggr] \\ & - \frac{2m_f^2}{(4\pi)^2}\biggl[\ln^2\biggl(\frac{\bar{\mu}e^{\gamma_{\rm E}}}{\pi T}\biggr) - \gamma_{\rm E}^2 - 2\ln^2(2) - 2\gamma_1 + \frac{\pi^2}{8}\biggr] + \mathcal{O}\biggl(\frac{m_f^4}{\pi^4 T^2}\biggr)\,. \end{aligned} \tag{A.19}$$

A.3. Function $I(\underline{m})$

The thermal 2-loop effective potential contains appearances of a "Lorentz-violating" 1-loop structure denoted by

$$I(\underline{m}) \equiv \sum\!\!\!\!\!\!\int_P \frac{p^2}{P^2 + m^2} = -\frac{D-1}{D}m^2 A(m) + \int_{\mathbf{p}} \frac{p^2 n(\omega)}{\omega}\,, \tag{A.20}$$

where the vacuum part A is from eq. (C.1). We write

$$I(\underline{m}) = \frac{1}{\epsilon} I^{(-1)}(\underline{m}) + I^{(0)}(\underline{m}) + \epsilon\, I^{(1)}(\underline{m}) + \mathcal{O}(\epsilon^2)\,, \tag{A.21}$$

and $I^{(n)}(\underline{m}) = I_0^{(n)}(\underline{m}) + I_T^{(n)}(\underline{m})$. Suppressing an overall $\mu^{-2\epsilon}$, the expressions for the structures in eq. (A.21) read

$$I^{(-1)}(\underline{m}) = \frac{3m^4}{4(4\pi)^2}\,, \tag{A.22}$$

$$I^{(0)}(\underline{m}) = \frac{m^4}{(4\pi)^2}\biggl(\frac{3}{4}\ln\frac{\bar{\mu}^2}{m^2} + \frac{5}{8}\biggr) + I_T^{(0)}(\underline{m})\,, \tag{A.23}$$

$$I_T^{(0)}(\underline{m}) = \int_0^\infty \frac{{\rm d}p\, p^4\, n(\omega)}{2\pi^2\omega}\,, \tag{A.24}$$

$$I^{(1)}(\underline{m}) = \frac{m^4}{(4\pi)^2}\biggl(\frac{3}{8}\ln^2\frac{\bar{\mu}^2}{m^2} + \frac{5}{8}\ln\frac{\bar{\mu}^2}{m^2} + \frac{9}{16} + \frac{\pi^2}{16}\biggr) + I_T^{(1)}(\underline{m})\,, \tag{A.25}$$

$$I_T^{(1)}(\underline{m}) = \int_0^\infty \frac{{\rm d}p\, p^4\,(\ln\frac{\bar{\mu}^2}{4p^2} + 2)n(\omega)}{2\pi^2\omega}\,. \tag{A.26}$$

These functions are related through $I^{(n)}(\underline{m}) = \bar{\mu}^2 \partial I^{(n+1)}(\underline{m})/\partial\bar{\mu}^2$. In the high-$T$ limit, the bosonic contributions read

$$I^{(0)}(\underline{m_b}) = \frac{\pi^2 T^4}{30} - \frac{m_b^2 T^2}{8} + \mathcal{O}\Big(\frac{m_b^3 T}{\pi}\Big)\,, \tag{A.27}$$

$$I^{(1)}(\underline{m_b}) = \frac{\pi^2 T^4}{15}\left[\ln\Big(\frac{\bar{\mu}e^{\gamma_{\rm E}}}{2T}\Big) - \frac{\zeta'(4)}{\zeta(4)} - \frac{5}{6}\right] - \frac{m_b^2 T^2}{4}\left[\ln\Big(\frac{\bar{\mu}e^{\gamma_{\rm E}}}{2T}\Big) - \frac{\zeta'(2)}{\zeta(2)} - \frac{1}{3}\right] + \mathcal{O}\Big(\frac{m_b^3 T}{\pi}\Big)\,, \tag{A.28}$$

whereas the corresponding fermionic expressions are

$$I^{(0)}(\underline{m_f}) = -\frac{7\pi^2 T^4}{240} + \frac{m_f^2 T^2}{16} + \mathcal{O}\Big(\frac{m_f^4}{\pi^4 T^2}\Big)\,, \tag{A.29}$$

$$I^{(1)}(\underline{m_f}) = -\frac{7\pi^2 T^4}{120}\left[\ln\Big(\frac{\bar{\mu}e^{\gamma_{\rm E}}}{2T}\Big) - \frac{\zeta'(4)}{\zeta(4)} - \frac{\ln 2}{7} - \frac{5}{6}\right] + \frac{m_f^2 T^2}{8}\left[\ln\Big(\frac{\bar{\mu}e^{\gamma_{\rm E}}}{4T}\Big) - \frac{\zeta'(2)}{\zeta(2)} - \frac{1}{3}\right] + \mathcal{O}\Big(\frac{m_f^4}{\pi^2}\Big)\,. \tag{A.30}$$

A.4. Function $H(m_1, m_2, m_3)$

Next we consider the 2-loop "sunset" sum-integral,

$$H(m_1, m_2, m_3) \equiv \sum\!\!\!\!\!\!\int_{P,Q} \frac{1}{(P^2 + m_1^2)(Q^2 + m_2^2)[(P+Q)^2 + m_3^2]}\,. \tag{A.31}$$

The Matsubara sums can be carried out explicitly, and for the vacuum part the spatial integrations are also doable [84–86]. Writing the result as

$$H(\{m_i\}) \;=\; \frac{1}{\epsilon^2}\, H^{(-2)}(\{m_i\}) + \frac{1}{\epsilon}\, H^{(-1)}(\{m_i\}) + H^{(0)}(\{m_i\}) + \mathcal{O}(\epsilon)\,, \tag{A.32}$$

and omitting an overall $\mu^{-4\epsilon}$, the results read

$$H^{(-2)}(\{m_i\}) = -\frac{m_1^2 + m_2^2 + m_3^2}{2(4\pi)^4}\,, \tag{A.33}$$

$$H^{(-1)}(\{m_i\}) = -\frac{1}{(4\pi)^4}\sum_{i=1}^{3} m_i^2\left(\ln\frac{\bar{\mu}^2}{m_i^2} + \frac{3}{2}\right) \;+\; \sum_{i=1}^{3}\frac{I_T^{(0)}(m_i)}{(4\pi)^2}\,, \tag{A.34}$$

$$\begin{aligned} H^{(0)}(\{m_i\}) = \frac{1}{(4\pi)^4}\Bigg\{ & -\frac{1}{2}\sum_{i=1}^{3} m_i^2 \ln^2\Big(\frac{\bar{\mu}^2}{m_i^2}\Big) - 3\sum_{i=1}^{3} m_i^2 \ln\Big(\frac{\bar{\mu}^2}{m_i^2}\Big) - \Big(\frac{7}{2} + \frac{\pi^2}{12}\Big)\sum_{i=1}^{3} m_i^2 \\ & - \frac{1}{2}\Bigg[(m_1^2 + m_2^2 - m_3^2)\ln\Big(\frac{\bar{\mu}^2}{m_1^2}\Big)\ln\Big(\frac{\bar{\mu}^2}{m_2^2}\Big) \\ & + (m_1^2 + m_3^2 - m_2^2)\ln\Big(\frac{\bar{\mu}^2}{m_1^2}\Big)\ln\Big(\frac{\bar{\mu}^2}{m_3^2}\Big) \\ & + (m_2^2 + m_3^2 - m_1^2)\ln\Big(\frac{\bar{\mu}^2}{m_2^2}\Big)\ln\Big(\frac{\bar{\mu}^2}{m_3^2}\Big)\Bigg]\Bigg\} \end{aligned}$$

$$
\begin{aligned}
&+ R(m_1^2,m_2^2,m_3^2) L(m_1^2,m_2^2,m_3^2) \Big\} \\
&+ I_T^{(0)}(m_1)\,\mathrm{Re}\,B^{(0)}(-im_1;m_2,m_3) + I_T^{(0)}(m_2)\,\mathrm{Re}\,B^{(0)}(-im_2;m_3,m_1) \\
&+ I_T^{(0)}(m_3)\,\mathrm{Re}\,B^{(0)}(-im_3;m_1,m_2) + \sum_{i=1}^{3} \frac{I_T^{(1)}(m_i)}{(4\pi)^2} \\
&+ \int_0^\infty \frac{\mathrm{d}p\,\mathrm{d}q\; pq\, n(\omega_1^p) n(\omega_2^q)}{32\pi^4 \omega_1^p \omega_2^q} \ln\left| \frac{(m_3^2-m_1^2-m_2^2+2pq)^2 - 4(\omega_1^p)^2(\omega_2^q)^2}{(m_3^2-m_1^2-m_2^2-2pq)^2 - 4(\omega_1^p)^2(\omega_2^q)^2} \right| \\
&+ \int_0^\infty \frac{\mathrm{d}p\,\mathrm{d}q\; pq\, n(\omega_2^p) n(\omega_3^q)}{32\pi^4 \omega_2^p \omega_3^q} \ln\left| \frac{(m_1^2-m_2^2-m_3^2+2pq)^2 - 4(\omega_2^p)^2(\omega_3^q)^2}{(m_1^2-m_2^2-m_3^2-2pq)^2 - 4(\omega_2^p)^2(\omega_3^q)^2} \right| \\
&+ \int_0^\infty \frac{\mathrm{d}p\,\mathrm{d}q\; pq\, n(\omega_3^p) n(\omega_1^q)}{32\pi^4 \omega_3^p \omega_1^q} \ln\left| \frac{(m_2^2-m_3^2-m_1^2+2pq)^2 - 4(\omega_3^p)^2(\omega_1^q)^2}{(m_2^2-m_3^2-m_1^2-2pq)^2 - 4(\omega_3^p)^2(\omega_1^q)^2} \right| ,
\end{aligned}
\tag{A.35}
$$

where $\omega_i^p \equiv \sqrt{p^2+m_i^2}$ and $B^{(0)}$ is from eq. (C.12). For finite masses a representation of the undefined functions reads [86][4]

$$
R(m_1^2,m_2^2,m_3^2) = \sqrt{m_1^4+m_2^4+m_3^4-2m_1^2m_2^2-2m_1^2m_3^2-2m_2^2m_3^2}\,, \tag{A.36}
$$

$$
\begin{aligned}
L(m_1^2,m_2^2,m_3^2) = {} & \mathrm{Li}_2\Big(-\frac{t_3 m_2}{m_1}\Big) + \mathrm{Li}_2\Big(-\frac{t_3 m_1}{m_2}\Big) + \frac{\pi^2}{6} + \frac{\ln^2 t_3}{2} \\
& + \frac{1}{2}\bigg[\ln\Big(t_3+\frac{m_2}{m_1}\Big) - \ln\Big(t_3+\frac{m_1}{m_2}\Big) + \frac{3}{4}\ln\Big(\frac{m_1^2}{m_2^2}\Big)\bigg]\ln\Big(\frac{m_1^2}{m_2^2}\Big)\,,
\end{aligned}
\tag{A.37}
$$

$$
t_3 = \frac{m_3^2-m_1^2-m_2^2+R(m_1^2,m_2^2,m_3^2)}{2m_1m_2}\,. \tag{A.38}
$$

The functions $H^{(n)}$ are related through $H^{(n)}(\{m_i\}) = \frac{1}{2}\bar{\mu}^2\,\partial H^{(n+1)}(\{m_i\})/\partial\bar{\mu}^2$.

Given that the function H is always multiplied by $\sim g^2m^2$ in the effective potential, the order $\sim T^2$ in the high-T is sufficient for reaching the order $\sim g^2m^2T^2$ for V_2. To this accuracy (cf. e.g. refs. [87,88]),

$$
H(m_{b1},m_{b2},m_{b3}) = \frac{T^2}{(4\pi)^2}\bigg(\frac{1}{4\epsilon} + \ln\frac{\bar{\mu}}{m_{b1}+m_{b2}+m_{b3}} + \frac{1}{2}\bigg) + \mathcal{O}\Big(\frac{\epsilon T^2}{\pi^2}, \frac{m_{bi}T}{\pi^3}\Big)\,, \tag{A.39}
$$

$$
H(m_{b1},m_{f2},m_{f3}) = \mathcal{O}\Big(\frac{\epsilon T^2}{\pi^2}, \frac{m_{b1}T}{\pi^3}\Big)\,. \tag{A.40}
$$

[4] The function L is singular in certain limits, for instance $L(m^2,\epsilon^2,\epsilon^2) = -\pi^2/6 - 2\ln^2(m/\epsilon)$ for $\epsilon \to 0^+$.

A.5. Function $H(\underline{m_1}, m_2, m_3)$

The final ingredient needed is a variant of the "sunset" sum-integral in eq. (A.31), with one line weighted by an additional spatial momentum:

$$H(\underline{m_1}, m_2, m_3) \equiv \sum\!\!\!\!\!\!\int_{P,Q} \frac{p^2}{(P^2+m_1^2)(Q^2+m_2^2)[(P+Q)^2+m_3^2]} \,. \tag{A.41}$$

The Matsubara sums can be carried out as before, and for the vacuum parts Lorentz symmetry allows furthermore to write

$$H_0(\underline{m_1}, m_2, m_3) = \frac{D-1}{D}\Big[-m_1^2 H_0(m_1,m_2,m_3) + I_0(m_2) I_0(m_3)\Big] \,. \tag{A.42}$$

Expressing the result like in eq. (A.32) and omitting an overall $\mu^{-4\epsilon}$, we get

$$H^{(-2)}(\underline{m_1}, m_2, m_3) = \frac{3\big[m_1^2(m_1^2+m_2^2+m_3^2)+2m_2^2m_3^2\big]}{8(4\pi)^4} \,, \tag{A.43}$$

$$\begin{aligned}
&H^{(-1)}(\underline{m_1}, m_2, m_3) \\
&= \frac{17m_1^2(m_1^2+m_2^2+m_3^2)+22m_2^2m_3^2}{16(4\pi)^4} \\
&\quad + \frac{3}{4(4\pi)^4}\bigg[m_1^4\ln\Big(\frac{\bar\mu^2}{m_1^2}\Big) + m_2^2(m_1^2+m_3^2)\ln\Big(\frac{\bar\mu^2}{m_2^2}\Big) + m_3^2(m_1^2+m_2^2)\ln\Big(\frac{\bar\mu^2}{m_3^2}\Big)\bigg] \\
&\quad + \frac{1}{(4\pi)^2}\bigg\{I_T^{(0)}(\underline{m_1}) + \frac{1}{3}\Big[I_T^{(0)}(\underline{m_2}) + I_T^{(0)}(\underline{m_3})\Big]\bigg\} \\
&\quad + \frac{1}{4(4\pi)^2}\Big[(m_2^2-3m_1^2-3m_3^2)\,I_T^{(0)}(m_2) + (m_3^2-3m_1^2-3m_2^2)\,I_T^{(0)}(m_3)\Big] \,,
\end{aligned} \tag{A.44}$$

$$\begin{aligned}
&H^{(0)}(\underline{m_1}, m_2, m_3) \\
&= \frac{77\big[m_1^2(m_1^2+m_2^2+m_3^2)+62m_2^2m_3^2\big]}{32(4\pi)^4} + \frac{\pi^2\big[m_1^2(m_1^2+m_2^2+m_3^2)+2m_2^2m_3^2\big]}{16(4\pi)^4} \\
&\quad + \frac{3}{8(4\pi)^4}\bigg[m_1^4\ln^2\Big(\frac{\bar\mu^2}{m_1^2}\Big) + m_2^2(m_1^2+m_3^2)\ln^2\Big(\frac{\bar\mu^2}{m_2^2}\Big) + m_3^2(m_1^2+m_2^2)\ln^2\Big(\frac{\bar\mu^2}{m_3^2}\Big)\bigg] \\
&\quad + \frac{1}{8(4\pi)^4}\bigg[17m_1^4\ln\Big(\frac{\bar\mu^2}{m_1^2}\Big) + m_2^2(17m_1^2+11m_3^2)\ln\Big(\frac{\bar\mu^2}{m_2^2}\Big) \\
&\quad + m_3^2(17m_1^2+11m_2^2)\ln\Big(\frac{\bar\mu^2}{m_3^2}\Big)\bigg] \\
&\quad + \frac{1}{(4\pi)^4}\bigg\{\frac{3m_1^2}{8}\bigg[(m_1^2+m_2^2-m_3^2)\,\ln\Big(\frac{\bar\mu^2}{m_1^2}\Big)\ln\Big(\frac{\bar\mu^2}{m_2^2}\Big) \\
&\quad + (m_1^2+m_3^2-m_2^2)\,\ln\Big(\frac{\bar\mu^2}{m_1^2}\Big)\ln\Big(\frac{\bar\mu^2}{m_3^2}\Big) \\
&\quad + (m_2^2+m_3^2-m_1^2)\,\ln\Big(\frac{\bar\mu^2}{m_2^2}\Big)\ln\Big(\frac{\bar\mu^2}{m_3^2}\Big)\bigg] + \frac{3m_2^2m_3^2}{4}\ln\Big(\frac{\bar\mu^2}{m_2^2}\Big)\ln\Big(\frac{\bar\mu^2}{m_3^2}\Big)
\end{aligned}$$

$$
\begin{aligned}
&- \frac{3m_1^2}{4} R(m_1^2,m_2^2,m_3^2)\, L(m_1^2,m_2^2,m_3^2) \Bigg\} \\
&+ I_T^{(0)}(\underline{m_1})\, \mathrm{Re}\, B^{(0)}(-im_1;m_2,m_3) \\
&+ I_T^{(0)}(\underline{m_2}) \Bigg\{ \frac{R^2(m_1^2,m_2^2,m_3^2)+3m_1^2m_2^2}{3m_2^4}\, \mathrm{Re}\, B^{(0)}(-im_2;m_3,m_1) \\
&+ \frac{1}{18m_2^4(4\pi)^2}\Bigg[-6m_1^2(m_1^2+m_2^2-m_3^2)\ln\Big(\frac{\bar\mu^2}{m_1^2}\Big) + 6m_3^2(m_1^2+2m_2^2-m_3^2)\ln\Big(\frac{\bar\mu^2}{m_3^2}\Big) \\
&- 6m_1^4+m_2^4-6m_3^4-9m_1^2m_2^2+12m_1^2m_3^2+9m_2^2m_3^2\Bigg]\Bigg\} + (2\leftrightarrow 3) \\
&+ I_T^{(0)}(m_2) \Bigg\{ \frac{R^2(m_1^2,m_2^2,m_3^2)}{4m_2^2}\, \mathrm{Re}\, B^{(0)}(-im_2;m_3,m_1) \\
&- \frac{1}{4m_2^2(4\pi)^2}\Bigg[m_1^2(m_1^2+m_2^2-m_3^2)\ln\Big(\frac{\bar\mu^2}{m_1^2}\Big) + m_3^2(-m_1^2+m_2^2+m_3^2)\ln\Big(\frac{\bar\mu^2}{m_3^2}\Big) \\
&+ m_1^4+m_3^4+m_1^2m_2^2-2m_1^2m_3^2+m_2^2m_3^2\Bigg]\Bigg\} + (2\leftrightarrow 3) \\
&+ \frac{1}{(4\pi)^2}\Bigg\{ I_T^{(1)}(\underline{m_1}) + \frac{1}{3}\Big[I_T^{(1)}(\underline{m_2}) + I_T^{(1)}(\underline{m_3})\Big]\Bigg\} \\
&+ \frac{1}{4(4\pi)^2}\Big[(m_2^2-3m_1^2-3m_3^2)\, I_T^{(1)}(m_2) + (m_3^2-3m_1^2-3m_2^2)\, I_T^{(1)}(m_3)\Big] \\
&+ \int_0^\infty \frac{\mathrm{d}p\,\mathrm{d}q\; p^3 q\, n(\omega_1^p) n(\omega_2^q)}{32\pi^4\omega_1^p\omega_2^q} \ln\Bigg| \frac{(m_3^2-m_1^2-m_2^2+2pq)^2-4(\omega_1^p)^2(\omega_2^q)^2}{(m_3^2-m_1^2-m_2^2-2pq)^2-4(\omega_1^p)^2(\omega_2^q)^2}\Bigg| + (2\leftrightarrow 3) \\
&+ \int_0^\infty \frac{\mathrm{d}p\,\mathrm{d}q\; p^2 q^2\, n(\omega_2^p) n(\omega_3^q)}{4\pi^4\omega_2^p\omega_3^q} \Bigg\{ 1 + \frac{\omega_2^p\omega_3^q}{4pq} \ln\Bigg| \frac{(m_1^2-m_2^2-m_3^2)^2-4(pq-\omega_2^p\omega_3^q)^2}{(m_1^2-m_2^2-m_3^2)^2-4(pq+\omega_2^p\omega_3^q)^2}\Bigg| \\
&+ \frac{(\omega_2^p)^2+(\omega_3^q)^2-m_1^2}{8pq} \ln\Bigg| \frac{(m_1^2-m_2^2-m_3^2+2pq)^2-4(\omega_2^p)^2(\omega_3^q)^2}{(m_1^2-m_2^2-m_3^2-2pq)^2-4(\omega_2^p)^2(\omega_3^q)^2}\Bigg|\Bigg\}\,, \qquad \text{(A.45)}
\end{aligned}
$$

where $\omega_i^p \equiv \sqrt{p^2+m_i^2}$, $B^{(0)}$ is from eq. (C.12), and R and L are from eqs. (A.36) and (A.37), respectively. The functions are related through $H^{(n)} = \frac{1}{2}\bar\mu^2\,\partial H^{(n+1)}/\partial\bar\mu^2$.

The numerical evaluation of eq. (A.45) is straightforward if all masses are of similar orders of magnitude. In contrast, if there is a hierarchy between the masses (cf. e.g. eq. (B.14)), care must be taken in order to avoid significance loss in the numerics. For instance, the coefficient multiplying $I_T^{(0)}(\underline{m_2})$ has a finite limit for $m_2 \to 0$, but many individual terms within the curly brackets diverge as $\sim 1/m_2^4$. A similar problem appears in the coefficient multiplying $I_T^{(0)}(m_2)$, even though divergences are only $\sim 1/m_2^2$ in this case. It may also be noted that the coefficients of $I_T^{(0)}(\underline{m_2})$ and $I_T^{(0)}(m_2)$ have cusps at $m_2 = m_1 + m_3$, originating from the function $B^{(0)}$, which cancel against corresponding cusps originating from the last three rows of eq. (A.45). For a proper cancellation of the cusps, all terms involved need to be evaluated with good precision.

A powerful crosscheck on the numerics is provided by the high-T limit, which can be given in analytic form (cf. eqs. (A.46)–(A.48)).

In the high-T limit, making use of relations determined in ref. [89],[5] we get

$$H(\underline{m_{b1}}, m_{b2}, m_{b3}) = \frac{T^4}{72}\left[\frac{1}{4\epsilon} + \ln\left(\frac{\bar{\mu}e^{\gamma_{\rm E}}}{2T}\right) - \frac{\zeta'(2)}{\zeta(2)}\right] + \frac{D-1}{2} I(0_b)\left[I_{n=0}(m_{b2}) + I_{n=0}(m_{b3})\right] + \frac{m_{2b}m_{3b}T^2}{(4\pi)^2} - \frac{m_{1b}^2 T^2}{(4\pi)^2}\left[\frac{1}{4\epsilon} + \ln\left(\frac{\bar{\mu}}{m_{b1}+m_{b2}+m_{b3}}\right) + \frac{1}{2}\right] + \mathcal{O}\left(\epsilon T^4, \frac{m^2T^2}{\pi^2}\right), \tag{A.46}$$

$$H(\underline{m_{b1}}, m_{f2}, m_{f3}) = \frac{T^4}{288}\left[\frac{1}{4\epsilon} + \ln\left(\frac{\bar{\mu}e^{\gamma_{\rm E}}}{4T}\right) - \frac{\zeta'(2)}{\zeta(2)}\right] + \mathcal{O}\left(\epsilon T^4, \frac{m^2T^2}{\pi^2}\right), \tag{A.47}$$

$$H(\underline{m_{f1}}, m_{f2}, m_{b3}) = -\frac{T^4}{144}\left[\frac{1}{4\epsilon} + \ln\left(\frac{\bar{\mu}e^{\gamma_{\rm E}}}{T}\right) - \frac{3\ln(2)}{2} - \frac{\zeta'(2)}{\zeta(2)}\right] + \frac{D-1}{2} I(0_f)\, I_{n=0}(m_{b3}) + \mathcal{O}\left(\epsilon T^4, \frac{m^2T^2}{\pi^2}\right). \tag{A.48}$$

Here the so-called linear terms, of the type $\mathcal{O}(mT^3)$, have been written in a D-dimensional form, permitting for a crosscheck of their D-dimensional cancellation in the full result (cf. the discussion around the end of sec. 3).

The function $H(\underline{m_1}, m_2, m_3)$ always appears in a difference containing various masses, so that the leading term $\propto T^4$ of the high-T expansion drops out from the effective potential. Moreover, at $\mathcal{O}(m^2)$, only the *non-analytic terms* originating from Matsubara zero modes have been kept in the expressions above, given that analytic terms lead to v-independent structures of the type $\sim g^2(\widetilde{m}_W^2 - m_W^2)T^2 \sim g^4T^4$.

Appendix B. 2-loop diagrams

In order to list all contributions to V_2, we make use of the master sum-integrals defined in Appendices A.2–A.5 The diagrams are of three types, illustrated in Fig. 1. We denote the particles circling in the loops by scalar (s), vector (v), ghost (g), or fermion (f). Then the various contributions read (some v-independent terms have been dropped for simplicity)

$$\begin{aligned}
(\mathrm{sss}) = {} & -3v^2\lambda_1^2\left[H(\widetilde{m}_h, \widetilde{m}_h, \widetilde{m}_h) + H(\widetilde{m}_h, \widetilde{m}_G, \widetilde{m}_G)\right] \\
& - \frac{v^2}{4}\left[(\lambda_3+\lambda_4+\lambda_5)^2 H(\widetilde{m}_h, \widetilde{m}_H, \widetilde{m}_H) + (\lambda_3+\lambda_4-\lambda_5)^2 H(\widetilde{m}_h, \widetilde{m}_A, \widetilde{m}_A)\right] \\
& - \frac{v^2}{4}\left[(\lambda_4+\lambda_5)^2 H(\widetilde{m}_G, \widetilde{m}_H, \widetilde{m}_{H_\pm}) + (\lambda_4-\lambda_5)^2 H(\widetilde{m}_G, \widetilde{m}_A, \widetilde{m}_{H_\pm})\right] \\
& - \frac{v^2}{2}\left[\lambda_3^2\, H(\widetilde{m}_h, \widetilde{m}_{H_\pm}, \widetilde{m}_{H_\pm}) + \lambda_5^2\, H(\widetilde{m}_G, \widetilde{m}_H, \widetilde{m}_A)\right],
\end{aligned} \tag{B.1}$$

[5] We thank Y. Schröder for locating the necessary relations.

$$
\begin{aligned}
(\mathrm{ss}) = {} & \frac{3\lambda_1}{4}\big[I^2(\widetilde{m}_h) + 2I(\widetilde{m}_h)I(\widetilde{m}_G) + 5I^2(\widetilde{m}_G)\big] \\
& + \frac{\lambda_2}{2}\big[I^2(\widetilde{m}_H) + I^2(\widetilde{m}_A) + 2I^2(\widetilde{m}_{H_\pm})\big] + \frac{\lambda_2}{4}\big[I(\widetilde{m}_H) + I(\widetilde{m}_A) + 2I(\widetilde{m}_{H_\pm})\big]^2 \\
& + \frac{\lambda_3+\lambda_4+\lambda_5}{4}\big[I(\widetilde{m}_h)I(\widetilde{m}_H) + I(\widetilde{m}_G)I(\widetilde{m}_A)\big] \\
& + \frac{\lambda_3+\lambda_4-\lambda_5}{4}\big[I(\widetilde{m}_h)I(\widetilde{m}_A) + I(\widetilde{m}_G)I(\widetilde{m}_H)\big] \\
& + (\lambda_3+\lambda_4)I(\widetilde{m}_G)I(\widetilde{m}_{H_\pm}) \\
& + \frac{\lambda_3}{2}\big\{I(\widetilde{m}_h)I(\widetilde{m}_{H_\pm}) + I(\widetilde{m}_G)\big[I(\widetilde{m}_H) + I(\widetilde{m}_A) + I(\widetilde{m}_{H_\pm})\big]\big\}\,, \qquad \text{(B.2)}
\end{aligned}
$$

$$
\begin{aligned}
(\mathrm{s}) = {} & \frac{\delta m_h^2 - \delta m_{\phi T}^2 - \widetilde{m}_h^2\delta Z_\phi}{2}\, I(\widetilde{m}_h) + \frac{3(\delta m_G^2 - \delta m_{\phi T}^2 - \widetilde{m}_G^2\delta Z_\phi)}{2}\, I(\widetilde{m}_G) \\
& + \frac{\delta m_H^2 - \delta m_{\chi T}^2 - \widetilde{m}_H^2\delta Z_\chi}{2}\, I(\widetilde{m}_H) + \frac{\delta m_A^2 - \delta m_{\chi T}^2 - \widetilde{m}_A^2\delta Z_\chi}{2}\, I(\widetilde{m}_A) \\
& + \big(\delta m_{H_\pm}^2 - \delta m_{\chi T}^2 - \widetilde{m}_{H_\pm}^2\delta Z_\chi\big)\, I(\widetilde{m}_{H_\pm})\,, \qquad \text{(B.3)}
\end{aligned}
$$

$$
\begin{aligned}
(\mathrm{ssv}) = {} & -\frac{3g_2^2}{8}\Big\{(\widetilde{m}_W^2 - 2\widetilde{m}_h^2 - 2\widetilde{m}_G^2)H(\widetilde{m}_W,\widetilde{m}_h,\widetilde{m}_G) \\
& + (\widetilde{m}_W^2 - 4\widetilde{m}_G^2)H(\widetilde{m}_W,\widetilde{m}_G,\widetilde{m}_G) \\
& - \big[I(\widetilde{m}_h) + I(\widetilde{m}_G)\big]I(\widetilde{m}_G) + 2\big[I(\widetilde{m}_h) + 3I(\widetilde{m}_G)\big]I(\widetilde{m}_W) \\
& + H(\underline{\widetilde{m}_W},\widetilde{m}_h,\widetilde{m}_G) - 2H(\widetilde{m}_W,\underline{\widetilde{m}_h},\widetilde{m}_G) - 2H(\widetilde{m}_W,\widetilde{m}_h,\underline{\widetilde{m}_G}) \\
& + H(\underline{\widetilde{m}_W},\widetilde{m}_G,\widetilde{m}_G) - 4H(\widetilde{m}_W,\underline{\widetilde{m}_G},\widetilde{m}_G) \\
& - H(\underline{m_W},\widetilde{m}_h,\widetilde{m}_G) + 2H(m_W,\underline{\widetilde{m}_h},\widetilde{m}_G) + 2H(m_W,\widetilde{m}_h,\underline{\widetilde{m}_G}) \\
& - H(\underline{m_W},\widetilde{m}_G,\widetilde{m}_G) + 4H(m_W,\underline{\widetilde{m}_G},\widetilde{m}_G)\Big\} \\
& - \frac{g_2^2}{8}\Big\{(\widetilde{m}_W^2 - 2\widetilde{m}_H^2 - 2\widetilde{m}_A^2)H(\widetilde{m}_W,\widetilde{m}_H,\widetilde{m}_A) \\
& + (\widetilde{m}_W^2 - 4\widetilde{m}_{H_\pm}^2)H(\widetilde{m}_W,\widetilde{m}_{H_\pm},\widetilde{m}_{H_\pm}) \\
& + 2(\widetilde{m}_W^2 - 2\widetilde{m}_H^2 - 2\widetilde{m}_{H_\pm}^2)H(\widetilde{m}_W,\widetilde{m}_H,\widetilde{m}_{H_\pm}) \\
& + 2(\widetilde{m}_W^2 - 2\widetilde{m}_A^2 - 2\widetilde{m}_{H_\pm}^2)H(\widetilde{m}_W,\widetilde{m}_A,\widetilde{m}_{H_\pm}) \\
& - I(\widetilde{m}_H)I(\widetilde{m}_A) - \big[2I(\widetilde{m}_H) + 2I(\widetilde{m}_A) + I(\widetilde{m}_{H_\pm})\big]I(\widetilde{m}_{H_\pm}) \\
& + 6\big[I(\widetilde{m}_H) + I(\widetilde{m}_A) + 2I(\widetilde{m}_{H_\pm})\big]I(\widetilde{m}_W) \\
& + H(\underline{\widetilde{m}_W},\widetilde{m}_H,\widetilde{m}_A) - 2H(\widetilde{m}_W,\underline{\widetilde{m}_H},\widetilde{m}_A) - 2H(\widetilde{m}_W,\widetilde{m}_H,\underline{\widetilde{m}_A}) \\
& + 2H(\underline{\widetilde{m}_W},\widetilde{m}_H,\widetilde{m}_{H_\pm}) - 4H(\widetilde{m}_W,\underline{\widetilde{m}_H},\widetilde{m}_{H_\pm}) - 4H(\widetilde{m}_W,\widetilde{m}_H,\underline{\widetilde{m}_{H_\pm}}) \\
& + 2H(\underline{\widetilde{m}_W},\widetilde{m}_A,\widetilde{m}_{H_\pm}) - 4H(\widetilde{m}_W,\underline{\widetilde{m}_A},\widetilde{m}_{H_\pm}) - 4H(\widetilde{m}_W,\widetilde{m}_A,\underline{\widetilde{m}_{H_\pm}}) \\
& + H(\underline{\widetilde{m}_W},\widetilde{m}_{H_\pm},\widetilde{m}_{H_\pm}) - 4H(\widetilde{m}_W,\underline{\widetilde{m}_{H_\pm}},\widetilde{m}_{H_\pm}) \\
& - H(\underline{m_W},\widetilde{m}_H,\widetilde{m}_A) + 2H(m_W,\underline{\widetilde{m}_H},\widetilde{m}_A) + 2H(m_W,\widetilde{m}_H,\underline{\widetilde{m}_A}) \\
& - 2H(\underline{m_W},\widetilde{m}_H,\widetilde{m}_{H_\pm}) + 4H(m_W,\underline{\widetilde{m}_H},\widetilde{m}_{H_\pm}) + 4H(m_W,\widetilde{m}_H,\underline{\widetilde{m}_{H_\pm}}) \\
& - 2H(\underline{m_W},\widetilde{m}_A,\widetilde{m}_{H_\pm}) + 4H(m_W,\underline{\widetilde{m}_A},\widetilde{m}_{H_\pm}) + 4H(m_W,\widetilde{m}_A,\underline{\widetilde{m}_{H_\pm}})
\end{aligned}
$$

$$- H(\underline{m_W}, \widetilde{m}_{H_\pm}, \widetilde{m}_{H_\pm}) + 4H(m_W, \underline{\widetilde{m}_{H_\pm}}, \widetilde{m}_{H_\pm}) \Big\} \,, \tag{B.4}$$

$$(\mathrm{sv}) = \frac{3g_2^2}{8}\big[I(\widetilde{m}_h) + 3I(\widetilde{m}_G)\big]\big[I(\widetilde{m}_W) + (D-1)I(m_W)\big]$$
$$+ \frac{3g_2^2}{8}\big[I(\widetilde{m}_H) + I(\widetilde{m}_A) + 2I(\widetilde{m}_{H_\pm})\big]\big[I(\widetilde{m}_W) + (D-1)I(m_W)\big] \,, \tag{B.5}$$

$$(\mathrm{svv}) = -\frac{3g_2^2 m_W^2}{4}\big[H(\widetilde{m}_h, \widetilde{m}_W, \widetilde{m}_W) + (D-1)H(\widetilde{m}_h, m_W, m_W)\big] \,, \tag{B.6}$$

$$(\mathrm{sgg}) = \frac{3g_2^2 m_W^2}{8}\big[H(\widetilde{m}_h, m_W, m_W) - 2H(\widetilde{m}_G, m_W, m_W)\big] \,, \tag{B.7}$$

$$(\mathrm{vvv}) = -\frac{3g_2^2}{2}\Big\{(D-1)(\widetilde{m}_W^2 - 4m_W^2)H(\widetilde{m}_W, m_W, m_W)$$
$$+ (D-1)\big[4I(\widetilde{m}_W) - I(m_W)\big]I(m_W) + (D-1)\big[H(\underline{\widetilde{m}_W}, m_W, m_W)$$
$$- 4H(\widetilde{m}_W, \underline{m_W}, m_W) + 3H(\underline{m_W}, m_W, m_W)\big]$$
$$- H(\underline{m_W}, \widetilde{m}_W, \widetilde{m}_W) + 4H(m_W, \underline{\widetilde{m}_W}, \widetilde{m}_W) - 3H(\underline{m_W}, m_W, m_W)\Big\} \,, \tag{B.8}$$

$$(\mathrm{ggv}) = -\frac{3g_2^2}{2}\Big\{(2m_W^2 - \widetilde{m}_W^2)H(\widetilde{m}_W, m_W, m_W) + \big[I(m_W) - 2I(\widetilde{m}_W)\big]I(m_W)$$
$$- H(\underline{\widetilde{m}_W}, m_W, m_W) + 2H(\widetilde{m}_W, \underline{m_W}, m_W) - H(\underline{m_W}, m_W, m_W)\Big\} \,, \tag{B.9}$$

$$(\mathrm{vv}) = \frac{3g_2^2}{2}(D-1)\big[2I(\widetilde{m}_W) + (D-2)I(m_W)\big]I(m_W) \,, \tag{B.10}$$

$$(\mathrm{v}) = \frac{3}{2}\Big\{\delta Z_\xi\big[I(\underline{\widetilde{m}_W}) - I(\underline{m_W})\big] + (D-1)m_W^2(\delta Z_{g^2} + \delta Z_\phi)\, I(m_W)$$
$$+ \big[\widetilde{m}_W^2 \delta Z_\xi - m_{\mathrm{E}2}^2 \delta Z_A + m_W^2(\delta Z_{g^2} + \delta Z_\phi)\big] I(\widetilde{m}_W)\Big\} - \frac{3}{2}m_{\mathrm{E}2}^2 I(\widetilde{m}_W) \,, \tag{B.11}$$

$$(\mathrm{g}) = -3m_W^2\left(\delta Z_\xi + \delta Z_{g^2} + \frac{\delta Z_\phi + \delta Z_v}{2}\right) I(m_W) \,, \tag{B.12}$$

$$(\mathrm{sff}) = -\frac{3h_t^2}{2}\Big\{(\widetilde{m}_h^2 - 4m_t^2)H(\widetilde{m}_h, m_t, m_t) + \widetilde{m}_G^2 H(\widetilde{m}_G, m_t, m_t)$$
$$+ 2(\widetilde{m}_G^2 - m_t^2)H(\widetilde{m}_G, m_t, 0_f) - 2\big[I(m_t) + I(0_f)\big]I(m_t)$$
$$+ 2I(\widetilde{m}_h)I(m_t) + 2I(\widetilde{m}_G)\big[I(0_f) + 2I(m_t)\big]\Big\} \,, \tag{B.13}$$

$$(\mathrm{gff}) = \frac{3g_2^2}{8}\Big\{(\widetilde{m}_W^2 - 2m_t^2)H(\widetilde{m}_W, m_t, m_t) - (D-1)(m_W^2 - 2m_t^2)H(m_W, m_t, m_t)$$
$$+ (D-2)I^2(m_t) + 2\big[I(\widetilde{m}_W) - (D-1)I(m_W)\big]I(m_t)$$
$$- 2H(\underline{m_W}, m_t, m_t) + 4H(m_W, \underline{m_t}, m_t) + 2H(\underline{\widetilde{m}_W}, m_t, m_t)$$
$$- 4H(\widetilde{m}_W, \underline{m_t}, m_t)\Big\}$$
$$+ \frac{3g_2^2}{2}\Big\{(\widetilde{m}_W^2 - m_t^2)H(\widetilde{m}_W, m_t, 0_f) - (D-1)(m_W^2 - m_t^2)H(m_W, m_t, 0_f)$$
$$+ (D-2)I(m_t)I(0_f) + \big[I(\widetilde{m}_W) - (D-1)I(m_W)\big]\big[I(m_t) + I(0_f)\big]$$

$$
\begin{aligned}
&- 2H(\underline{m_W}, m_t, 0_f) + 2H(m_W, \underline{m_t}, 0_f) + 2H(m_W, m_t, \underline{0_f}) \\
&+ 2H(\underline{\widetilde{m}_W}, m_t, 0_f) - 2H(\widetilde{m}_W, \underline{m_t}, 0_f) - 2H(\widetilde{m}_W, m_t, \underline{0_f}) \Big\} \\
&+ \frac{3(8n_G-5)g_2^2}{8} \Big\{ \widetilde{m}_W^2 H(\widetilde{m}_W, 0_f, 0_f) - (D-1) m_W^2 H(m_W, 0_f, 0_f) \\
&+ (D-2) I^2(0_f) + 2\big[I(\widetilde{m}_W) - (D-1) I(m_W) \big] I(0_f) \\
&- 2H(\underline{m_W}, 0_f, 0_f) + 4H(m_W, \underline{0_f}, 0_f) \\
&+ 2H(\underline{\widetilde{m}_W}, 0_f, 0_f) - 4H(\widetilde{m}_W, \underline{0_f}, 0_f) \Big\} \\
&+ 4g_3^2 \Big\{ (m_{\rm E3}^2 - 4m_t^2) H(m_{\rm E3}, m_t, m_t) \\
&+ (D-2) I^2(m_t) + 2\big[I(m_{\rm E3}) - (D-1) I(0_b) \big] I(m_t) \\
&- 2H(\underline{0_b}, m_t, m_t) + 4H(0_b, \underline{m_t}, m_t) \\
&+ 2H(\underline{m_{\rm E3}}, m_t, m_t) - 4H(m_{\rm E3}, \underline{m_t}, m_t) \Big\} \,, \qquad \text{(B.14)}
\end{aligned}
$$

$$
\text{(f)} = -6m_t^2 \big(\delta Z_\phi + \delta Z_{h_t^2} \big) I(m_t) \,. \qquad \text{(B.15)}
$$

Appendix C. Vacuum renormalization

For the thermal computations, we need to know the running couplings as functions of the $\overline{\rm MS}$ scale $\bar{\mu}$ up to a scale $\bar{\mu} \sim \pi T$, cf. eq. (5.5). These can be obtained from renormalization group equations, provided that the initial values are known at some scale $\bar{\mu} \sim m_Z$. In order to obtain the latter, we compute physical pole masses and the Fermi constant in terms of the $\overline{\rm MS}$ parameters, and then invert the relations in order to express the $\overline{\rm MS}$ couplings at $\bar{\mu} = m_Z$ in terms of the physical ones. For the Standard Model, these relations were determined up to 1-loop level in ref. [55],[6] and here we extend the relations to the IDM. Closely related expressions for the IDM can be found in ref. [14].

C.1. Basis functions

In order to display the results for physical quantities, we make use of standard Passarino–Veltman type functions, which we have defined in Euclidean spacetime:

$$
A(m) \equiv \int_P \frac{1}{P^2 + m^2} \,, \qquad \text{(C.1)}
$$

$$
B(K; m_1, m_2) \equiv \int_P \frac{1}{[(P+K)^2 + m_1^2](P^2 + m_2^2)} \,, \qquad \text{(C.2)}
$$

$$
K_\mu C(K; m_1, m_2) \equiv \int_P \frac{P_\mu}{[(P+K)^2 + m_1^2](P^2 + m_2^2)} \,, \qquad \text{(C.3)}
$$

$$
C(K; m_1, m_2) = \frac{1}{2K^2} \big[A(m_2) - A(m_1) - (K^2 + m_1^2 - m_2^2)\, B(K; m_1, m_2) \big] \,, \qquad \text{(C.4)}
$$

[6] In eq. (193) of ref. [55], there is a term $-\frac{8}{3} t^2 \ln h$ missing from within the square brackets.

$$D_{\mu\nu}(K;m_1,m_2) \equiv \int_P \frac{P_\mu P_\nu}{[(P+K)^2+m_1^2](P^2+m_2^2)} \tag{C.5}$$

$$\begin{aligned} &= \frac{\delta_{\mu\nu} - \frac{D\,K_\mu K_\nu}{K^2}}{4(D-1)K^2}\Big\{(K^2-m_1^2+m_2^2)\,A(m_1) + (K^2+m_1^2-m_2^2)\,A(m_2) \\ &\quad - \big[K^4 + 2K^2(m_1^2+m_2^2) + (m_1^2-m_2^2)^2\big]B(K;m_1,m_2)\Big\} \\ &\quad + \frac{K_\mu K_\nu}{K^2}\big[A(m_1) - m_2^2\,B(K;m_1,m_2)\big]\,. \end{aligned} \tag{C.6}$$

For $D = 4-2\epsilon$ and writing $A = \sum_{n=-1}^{\infty} A^{(n)}\epsilon^n$ etc., the divergent parts of these functions can be expressed as

$$A^{(-1)}(m) = \frac{\mu^{-2\epsilon}}{(4\pi)^2}\big(-m^2\big)\,, \tag{C.7}$$

$$B^{(-1)}(K;m_1,m_2) = \frac{\mu^{-2\epsilon}}{(4\pi)^2}\,, \tag{C.8}$$

$$C^{(-1)}(K;m_1,m_2) = \frac{\mu^{-2\epsilon}}{(4\pi)^2}\left(-\frac{1}{2}\right), \tag{C.9}$$

$$D_{\mu\nu}^{(-1)}(K;m_1,m_2) = \frac{\mu^{-2\epsilon}}{(4\pi)^2}\left(-\frac{K^2+3m_1^2+3m_2^2}{12}\,\delta_{\mu\nu} + \frac{K_\mu K_\nu}{3}\right). \tag{C.10}$$

The finite parts of A and B read

$$A^{(0)}(m) = -\frac{m^2}{(4\pi)^2}\left(\ln\frac{\bar\mu^2}{m^2}+1\right), \tag{C.11}$$

$$\begin{aligned} B^{(0)}(K;m_1,m_2) = \frac{1}{(4\pi)^2}\Bigg[&\ln\frac{\bar\mu^2}{m_1 m_2} + 2 + \frac{m_1^2-m_2^2}{K^2}\ln\frac{m_1}{m_2} \\ &- \frac{2\sqrt{(m_1-m_2)^2+K^2}\sqrt{(m_1+m_2)^2+K^2}}{K^2} \\ &\times \operatorname{artanh}\left(\frac{\sqrt{(m_1-m_2)^2+K^2}}{\sqrt{(m_1+m_2)^2+K^2}}\right)\Bigg]. \end{aligned} \tag{C.12}$$

Given that $B^{(0)}$ is a function of K^2 only, we use an implicit notation in which K may denote either a vector or its modulus. The corresponding expressions after going to Minkowskian signature, i.e. $K \to -i\mathcal{K}$, are conventionally expressed in terms of a function F defined by

$$B^{(0)}(-i\mathcal{K};m_1,m_2) \equiv \frac{1}{(4\pi)^2}\left[\ln\frac{\bar\mu^2}{m_1 m_2} + 1 - \frac{m_1^2+m_2^2}{m_1^2-m_2^2}\ln\left(\frac{m_1}{m_2}\right) + F\left(\frac{m_1}{\mathcal{K}},\frac{m_2}{\mathcal{K}}\right)\right]. \tag{C.13}$$

The (real part of) F is given in eq. (C.16) below.

C.2. Gauge coupling renormalization

The first quantity needed is the initial value of the $\mathrm{SU_L}(2)$ gauge coupling g_2^2 at the scale $\bar\mu \sim m_Z$. It can be expressed in terms of the Fermi constant. Including the contribution of the new scalar degrees of freedom through a function Δ (cf. eq. (C.15)) we get

$$g^2(\bar\mu) = g_0^2\biggl\{1 + \frac{g_0^2}{16\pi^2}\biggl[\biggl(\frac{4n_G}{3} - 7\biggr)\ln\frac{\bar\mu^2}{m_W^2} + \Delta\Bigl(\frac{m_{H_\pm}}{m_W},\frac{m_H}{m_W}\Bigr) + \Delta\Bigl(\frac{m_{H_\pm}}{m_W},\frac{m_A}{m_W}\Bigr) - \frac{33}{4}F(1,1) + \frac{1}{12}(h^4 - 4h^2 + 12)\,\mathrm{Re}\,F(1,h) - \frac{1}{2}(t^4 + t^2 - 2)\,\mathrm{Re}\,F(t,0) - 2\ln t - \frac{h^2}{24} + \frac{t^2}{4} + \frac{20n_G}{9} - \frac{257}{72}\biggr]\biggr\}\,, \tag{C.14}$$

where $g_0^2 \equiv 4\sqrt{2}G_{\rm F}m_W^2$, $G_{\rm F} = 1.166379\times 10^{-5}\ \mathrm{GeV}^{-2}$ is the Fermi constant, $h \equiv m_h/m_W$, $t \equiv m_t/m_W$, the masses m_W, m_t, m_h, m_H, m_A and $m_{H_\pm}$ are the physical (vacuum) masses, and we have defined

$$\Delta(r_1,r_2) \equiv \frac{5}{36} - \frac{r_1^2+r_2^2}{24} - \frac{\ln(r_1r_2)}{12} + \frac{2r_1^2r_2^2 - r_1^2 - r_2^2}{12(r_1^2-r_2^2)}\ln\Bigl(\frac{r_1}{r_2}\Bigr) + \frac{(r_1^2-r_2^2)^2 - 2(r_1^2+r_2^2) + 1}{12}\,\mathrm{Re}\,F(r_1,r_2)\,. \tag{C.15}$$

Here the function F, defined in eq. (C.13), has the real part

$$\mathrm{Re}\,F(r_1,r_2) = 1 + \biggl(\frac{r_1^2+r_2^2}{r_1^2-r_2^2} + r_2^2 - r_1^2\biggr)\ln\Bigl(\frac{r_1}{r_2}\Bigr) - 2\,\mathrm{Re}\biggl[\sqrt{1-(r_1-r_2)^2}\sqrt{(r_1+r_2)^2-1}\,\arctan\frac{\sqrt{1-(r_1-r_2)^2}}{\sqrt{(r_1+r_2)^2-1}}\biggr]\,, \tag{C.16}$$

with the special limits

$$F(1,1) = 2 - \frac{\pi}{\sqrt{3}}\,, \tag{C.17}$$

$$\mathrm{Re}\,F(r,0) = 1 + (r^2-1)\ln\Bigl(1 - \frac{1}{r^2}\Bigr)\,, \quad r \geq 1\,. \tag{C.18}$$

C.3. Pole masses and scalar coupling renormalizations

The other couplings can be expressed in terms of pole masses. For this purpose we compute the full renormalized on-shell self-energies $\Pi(K;\bar\mu)$ of the neutral Higgs fields h; of the W boson; of the top quark; and of the new scalars H, A and $H^\pm$. For Standard Model particles the expressions read (here v_0 is the *tree-level* vacuum expectation value which can within the 1-loop expressions be approximated as $v_0^2 \equiv \mu_1^2(\bar\mu)/\lambda_1(\bar\mu) \approx 4m_W^2/g_0^2$):

$$\begin{aligned}
\Pi_h(-im_h;\bar\mu) &= m_h^2\,\delta Z_{\mu_1^2} \\
&+ 12h_t^2 A(m_t) - 6\lambda_1 A(m_h) + \biggl[\frac{3(1-D)g_2^2}{2} - 6\lambda_1\biggr]A(m_W) \\
&- 2\lambda_3 A(m_{H_\pm}) - \bigl(\lambda_3+\lambda_4+\lambda_5\bigr)A(m_H) - \bigl(\lambda_3+\lambda_4-\lambda_5\bigr)A(m_A) \\
&+ 3h_t^2(4m_t^2 - m_h^2)B(-im_h;m_t,m_t) - 9\lambda_1 m_h^2\,B(-im_h;m_h,m_h) \\
&+ \biggl\{\frac{3g_2^2}{2}\Bigl[(1-D)m_W^2 + m_h^2\Bigr] - 3\lambda_1 m_h^2\biggr\}B(-im_h;m_W,m_W) \\
&- \lambda_3^2 v_0^2\,B(-im_h;m_{H_\pm},m_{H_\pm}) - \frac{1}{2}\bigl(\lambda_3+\lambda_4+\lambda_5\bigr)^2 v_0^2\,B(-im_h;m_H,m_H)
\end{aligned}$$

$$- \frac{1}{2}\big(\lambda_3+\lambda_4-\lambda_5\big)^2 v_0^2\, B(-im_h; m_A, m_A)\,, \tag{C.19}$$

$$\begin{aligned}
\Pi_W^{(T)}(-im_W,\bar{\mu}) &= m_W^2\left(\delta Z_{g_2^2} - \delta Z_{\lambda_1} + \delta Z_{\mu_1^2}\right) \\
&+ g_2^2\Bigg\{\left(\frac{6m_t^2}{m_h^2}-\frac{3}{2}\right)A(m_t) - \frac{A(m_h)}{2} + \left[\frac{3(1-D)m_W^2}{2m_h^2}+2D-4\right]A(m_W) \\
&+ \left[\frac{1}{2}-\frac{\lambda_3 v_0^2}{2m_h^2}\right]A(m_{H_\pm}) \,+\, \left[\frac{1}{4}-\frac{(\lambda_3+\lambda_4+\lambda_5)v_0^2}{4m_h^2}\right]A(m_H) \\
&+ \left[\frac{1}{4}-\frac{(\lambda_3+\lambda_4-\lambda_5)v_0^2}{4m_h^2}\right]A(m_A) \\
&+ 6m_W^2 B(-im_W; m_W, m_W) - m_W^2 B(-im_W; m_W, m_h) \\
&+ \frac{3(m_t^2-m_W^2)}{2}\,B(-im_W;0,m_t) + \left(\frac{3}{2}-2n_G\right)m_W^2\,B(-im_W;0,0) \\
&+ \big(7-4D\big)\,D^{(T)}(-im_W;m_W,m_W) - D^{(T)}(-im_W;m_W,m_h) \\
&- D^{(T)}(-im_W;m_{H_\pm},m_H) \,-\, D^{(T)}(-im_W;m_{H_\pm},m_A) \\
&+ 6\,D^{(T)}(-im_W;0,m_t) \,+\, \big(8n_G-6\big)\,D^{(T)}(-im_W;0,0)\Bigg\}\,,
\end{aligned} \tag{C.20}$$

$$\begin{aligned}
2\big[\Sigma_{\rm s}(-im_t;\bar{\mu}) \,-\, \Sigma_{\rm v}(-im_t;\bar{\mu})\big] &= \delta Z_{h_t^2} - \delta Z_{\lambda_1} + \delta Z_{\mu_1^2} \\
&+ \frac{1}{m_h^2}\Bigg\{12h_t^2 A(m_t) - 6\lambda_1\,A(m_h) + \left[\frac{3(1-D)g_2^2}{2}-6\lambda_1\right]A(m_W) \\
&- 2\lambda_3\,A(m_{H_\pm}) \,-\, \big(\lambda_3+\lambda_4+\lambda_5\big)\,A(m_H) \,-\, \big(\lambda_3+\lambda_4-\lambda_5\big)\,A(m_A)\Bigg\} \\
&+ \frac{8Dg_3^2}{3}\,B(-im_t;0,m_t) + h_t^2\Big[B(-im_t;m_W,m_t) - B(-im_t;m_h,m_t)\Big] \\
&+ \frac{8(D-2)g_3^2}{3}\,C(-im_t;0,m_t) \\
&+ \frac{(D-2)g_2^2}{4}\Big[2C(-im_t;m_W,0) + C(-im_t;m_W,m_t)\Big] \\
&+ h_t^2\Big[C(-im_t;m_h,m_t) + C(-im_t;m_W,m_t) + C(-im_t;m_W,0)\Big]\,.
\end{aligned} \tag{C.21}$$

For W only the transverse parts play a role, and $D^{(T)}$ is defined by $D_{\mu\nu} \equiv D^{(T)}\delta_{\mu\nu} + \mathcal{O}(K_\mu K_\nu)$. In the case of the top quark the self-energy was expressed as $\Pi_t = i\not{K}\,\Sigma_{\rm v} + i\not{K}\gamma_5\Sigma_{\rm A} + m_t\,\Sigma_{\rm s}$; bracketing this with on-shell spinors eliminates the function $\Sigma_{\rm A}(K;\bar{\mu})$.

For the on-shell self-energies of the new scalars we obtain (denoting $n_3 = n_4 = -n_5 \equiv 1$)

$$\begin{aligned}
\Pi_H(-im_H;\bar{\mu}) \,&=\, \mu_2^2\,\delta Z_{\mu_2^2} + \sum_{i=3,4,5}\frac{\lambda_i v_0^2}{2}\big(\delta Z_{\lambda_i} + \delta Z_{\mu_1^2} - \delta Z_{\lambda_1}\big) \\
&+ \frac{12(\lambda_3+\lambda_4+\lambda_5)m_t^2}{m_h^2}\,A(m_t) \,-\, (\lambda_3+\lambda_4+\lambda_5)\,A(m_h)
\end{aligned}$$

$$
\begin{aligned}
&+\left[\frac{3(1-D)(\lambda_3+\lambda_4+\lambda_5)m_W^2}{m_h^2}+\frac{3(D-2)g_2^2}{4}-\lambda_4-2\lambda_5\right]A(m_W)\\
&+\left[3\lambda_2-\frac{(\lambda_3+\lambda_4+\lambda_5)^2v_0^2}{2m_h^2}\right]A(m_H)\\
&+\left[\lambda_2+\frac{g_2^2}{4}+\frac{\lambda_5^2v_0^2-(\lambda_3+\lambda_4)^2v_0^2}{2m_h^2}\right]A(m_A)\\
&+\left[2\lambda_2+\frac{g_2^2}{2}-\frac{\lambda_3(\lambda_3+\lambda_4+\lambda_5)v_0^2}{m_h^2}\right]A(m_{H_\pm})\\
&-(\lambda_3+\lambda_4+\lambda_5)^2v_0^2B(-im_H;m_h,m_H)\\
&-\left[\lambda_5^2v_0^2+\frac{(m_W^2-2m_H^2-2m_A^2)g_2^2}{4}\right]B(-im_H;m_W,m_A)\\
&-\left[\frac{(\lambda_4+\lambda_5)^2v_0^2}{2}+\frac{(m_W^2-2m_H^2-2m_{H_\pm}^2)g_2^2}{2}\right]B(-im_H;m_W,m_{H_\pm})\,, \qquad \text{(C.22)}
\end{aligned}
$$

$$
\begin{aligned}
\Pi_A(-im_A;\bar{\mu}) \;=\; &\mu_2^2\delta Z_{\mu_2^2}+\sum_{i=3,4,5}\frac{n_i\lambda_iv_0^2}{2}\big(\delta Z_{\lambda_i}+\delta Z_{\mu_1^2}-\delta Z_{\lambda_1}\big)\\
&+\frac{12(\lambda_3+\lambda_4-\lambda_5)m_t^2}{m_h^2}\,A(m_t)\;-\;(\lambda_3+\lambda_4-\lambda_5)\,A(m_h)\\
&+\left[\frac{3(1-D)(\lambda_3+\lambda_4-\lambda_5)m_W^2}{m_h^2}+\frac{3(D-2)g_2^2}{4}-\lambda_4+2\lambda_5\right]A(m_W)\\
&+\left[3\lambda_2-\frac{(\lambda_3+\lambda_4-\lambda_5)^2v_0^2}{2m_h^2}\right]A(m_A)\\
&+\left[\lambda_2+\frac{g_2^2}{4}+\frac{\lambda_5^2v_0^2-(\lambda_3+\lambda_4)^2v_0^2}{2m_h^2}\right]A(m_H)\\
&+\left[2\lambda_2+\frac{g_2^2}{2}-\frac{\lambda_3(\lambda_3+\lambda_4-\lambda_5)v_0^2}{m_h^2}\right]A(m_{H_\pm})\\
&-(\lambda_3+\lambda_4-\lambda_5)^2v_0^2B(-im_A;m_h,m_A)\\
&-\left[\lambda_5^2v_0^2+\frac{(m_W^2-2m_H^2-2m_A^2)g_2^2}{4}\right]B(-im_A;m_W,m_H)\\
&-\left[\frac{(\lambda_4-\lambda_5)^2v_0^2}{2}+\frac{(m_W^2-2m_A^2-2m_{H_\pm}^2)g_2^2}{2}\right]B(-im_A;m_W,m_{H_\pm})\,, \qquad \text{(C.23)}
\end{aligned}
$$

$$
\begin{aligned}
\Pi_{H_\pm}(-im_{H_\pm};\bar{\mu}) \;=\; &\mu_2^2\delta Z_{\mu_2^2}+\frac{\lambda_3v_0^2}{2}\big(\delta Z_{\lambda_3}+\delta Z_{\mu_1^2}-\delta Z_{\lambda_1}\big)\\
&+\frac{12\lambda_3m_t^2}{m_h^2}\,A(m_t)\;-\;\lambda_3\,A(m_h)\\
&+\left[\frac{3(1-D)\lambda_3m_W^2}{m_h^2}+\frac{3(D-2)g_2^2}{4}+\lambda_4\right]A(m_W)
\end{aligned}
$$

$$
\begin{aligned}
&+\left[\lambda_2+\frac{g_2^2}{4}-\frac{\lambda_3(\lambda_3+\lambda_4+\lambda_5)v_0^2}{2m_h^2}\right]A(m_H)\\
&+\left[\lambda_2+\frac{g_2^2}{4}-\frac{\lambda_3(\lambda_3+\lambda_4-\lambda_5)v_0^2}{2m_h^2}\right]A(m_A)\\
&+\left[4\lambda_2+\frac{g_2^2}{4}-\frac{\lambda_3^2v_0^2}{m_h^2}\right]A(m_{H_\pm})\;-\;\lambda_3^2v_0^2B(-im_{H_\pm};m_h,m_{H_\pm})\\
&-\left[\frac{(\lambda_4+\lambda_5)^2v_0^2}{4}+\frac{(m_W^2-2m_H^2-2m_{H_\pm}^2)g_2^2}{4}\right]B(-im_{H_\pm};m_W,m_H)\\
&-\left[\frac{(\lambda_4-\lambda_5)^2v_0^2}{4}+\frac{(m_W^2-2m_A^2-2m_{H_\pm}^2)g_2^2}{4}\right]B(-im_{H_\pm};m_W,m_A)\\
&-\left[\frac{(m_W^2-4m_{H_\pm}^2)g_2^2}{4}\right]B(-im_{H_\pm};m_W,m_{H_\pm})\,. \qquad \text{(C.24)}
\end{aligned}
$$

The on-shell self-energies correct tree-level masses, which can be expressed in terms of $\overline{\rm MS}$ parameters. For instance, the physical Higgs mass squared has the form $m_h^2=-2\mu_1^2(\bar\mu)+\mathrm{Re}\,\Pi_h(-im_h;\bar\mu)$. Here we defined the pole mass m_h through the projection of the complex pole to the real axis. The pole mass equation can be inverted to give

$$
\mu_1^2(\bar\mu)\quad\overset{\bar\mu\approx m_Z}{=}\quad-\frac{m_h^2}{2}\left[1-\frac{\mathrm{Re}\,\Pi_h(-im_h;\bar\mu)}{m_h^2}\right]. \qquad \text{(C.25)}
$$

Similarly, the other parameters read (always implicitly assuming $\bar\mu\approx m_Z$)

$$
\lambda_1(\bar\mu)=\frac{g_0^2m_h^2}{8m_W^2}\left[1+\frac{\delta g_2^2(\bar\mu)}{g_0^2}+\frac{\mathrm{Re}\,\Pi_W^{(T)}(-im_W;\bar\mu)}{m_W^2}-\frac{\mathrm{Re}\,\Pi_h(-im_h;\bar\mu)}{m_h^2}\right], \qquad \text{(C.26)}
$$

$$
h_t^2(\bar\mu)=\frac{g_0^2m_t^2}{2m_W^2}\left[1+\frac{\delta g_2^2(\bar\mu)}{g_0^2}+\frac{\mathrm{Re}\,\Pi_W^{(T)}(-im_W;\bar\mu)}{m_W^2}\;-\;2(\Sigma_{\rm s}-\Sigma_{\rm v})(-im_t;\bar\mu)\right], \qquad \text{(C.27)}
$$

$$
\begin{aligned}
\mu_2^2(\bar\mu)=&\,m_H^2\left[1-\frac{\mathrm{Re}\,\Pi_H(-im_H;\bar\mu)}{m_H^2}\right]\\
&-\frac{2\lambda_H(\bar\mu)m_W^2}{g_0^2}\left[1-\frac{\delta g_2^2(\bar\mu)}{g_0^2}-\frac{\mathrm{Re}\,\Pi_W^{(T)}(-im_W;\bar\mu)}{m_W^2}\right], \qquad \text{(C.28)}
\end{aligned}
$$

$$
\begin{aligned}
\lambda_3(\bar\mu)=&\,\frac{g_0^2m_{H_\pm}^2}{2m_W^2}\left[1+\frac{\delta g_2^2(\bar\mu)}{g_0^2}+\frac{\mathrm{Re}\,\Pi_W^{(T)}(-im_W;\bar\mu)}{m_W^2}-\frac{\mathrm{Re}\,\Pi_{H_\pm}(-im_{H_\pm};\bar\mu)}{m_{H_\pm}^2}\right]\\
&-\frac{g_0^2m_H^2}{2m_W^2}\left[1+\frac{\delta g_2^2(\bar\mu)}{g_0^2}+\frac{\mathrm{Re}\,\Pi_W^{(T)}(-im_W;\bar\mu)}{m_W^2}-\frac{\mathrm{Re}\,\Pi_H(-im_H;\bar\mu)}{m_H^2}\right]\\
&+\lambda_H(\bar\mu)\left[1-\frac{\delta g_2^2(\bar\mu)}{g_0^2}-\frac{\mathrm{Re}\,\Pi_W^{(T)}(-im_W;\bar\mu)}{m_W^2}\right], \qquad \text{(C.29)}
\end{aligned}
$$

$$
\lambda_4(\bar\mu)=\frac{g_0^2m_H^2}{4m_W^2}\left[1+\frac{\delta g_2^2(\bar\mu)}{g_0^2}+\frac{\mathrm{Re}\,\Pi_W^{(T)}(-im_W;\bar\mu)}{m_W^2}-\frac{\mathrm{Re}\,\Pi_H(-im_H;\bar\mu)}{m_H^2}\right]
$$

$$+\frac{g_0^2 m_A^2}{4m_W^2}\left[1+\frac{\delta g_2^2(\bar\mu)}{g_0^2}+\frac{\mathrm{Re}\,\Pi_W^{(T)}(-im_W;\bar\mu)}{m_W^2}-\frac{\mathrm{Re}\,\Pi_A(-im_A;\bar\mu)}{m_A^2}\right]$$
$$-\frac{g_0^2 m_{H_\pm}^2}{2m_W^2}\left[1+\frac{\delta g_2^2(\bar\mu)}{g_0^2}+\frac{\mathrm{Re}\,\Pi_W^{(T)}(-im_W;\bar\mu)}{m_W^2}-\frac{\mathrm{Re}\,\Pi_{H_\pm}(-im_{H_\pm};\bar\mu)}{m_{H_\pm}^2}\right]$$
$$+\frac{\lambda_H(\bar\mu)}{2}\left[\frac{\delta g_2^2(\bar\mu)}{g_0^2}+\frac{\mathrm{Re}\,\Pi_W^{(T)}(-im_W;\bar\mu)}{m_W^2}\right], \tag{C.30}$$

$$\lambda_5(\bar\mu)=\frac{g_0^2 m_H^2}{4m_W^2}\left[1+\frac{\delta g_2^2(\bar\mu)}{g_0^2}+\frac{\mathrm{Re}\,\Pi_W^{(T)}(-im_W;\bar\mu)}{m_W^2}-\frac{\mathrm{Re}\,\Pi_H(-im_H;\bar\mu)}{m_H^2}\right]$$
$$-\frac{g_0^2 m_A^2}{4m_W^2}\left[1+\frac{\delta g_2^2(\bar\mu)}{g_0^2}+\frac{\mathrm{Re}\,\Pi_W^{(T)}(-im_W;\bar\mu)}{m_W^2}-\frac{\mathrm{Re}\,\Pi_A(-im_A;\bar\mu)}{m_A^2}\right]$$
$$+\frac{\lambda_H(\bar\mu)}{2}\left[\frac{\delta g_2^2(\bar\mu)}{g_0^2}+\frac{\mathrm{Re}\,\Pi_W^{(T)}(-im_W;\bar\mu)}{m_W^2}\right], \tag{C.31}$$

where $\delta g_2^2(\bar\mu)\equiv g_2^2(\bar\mu)-g_0^2$ is from eq. (C.14). Following conventions in the literature, $\lambda_2(m_Z)$ and $\lambda_H(m_Z)\equiv\lambda_3(m_Z)+\lambda_4(m_Z)+\lambda_5(m_Z)$ are used directly as input parameters.

For approximate estimates, including only the large effects from λ_3^2, $(\lambda_3+\lambda_4\pm\lambda_5)^2$ and h_t^4, eqs. (C.25) and (C.26) can be simplified into

$$\mu_1^2(\bar\mu)\simeq -\frac{m_h^2}{2}+\frac{1}{32\pi^2}\left[2\lambda_3\left(m_{H_\pm}^2+\mu_2^2\ln\frac{\bar\mu^2}{m_{H_\pm}^2}\right)-12h_t^2m_t^2\right. \tag{C.32}$$
$$\left.+(\lambda_3+\lambda_4+\lambda_5)\left(m_H^2+\mu_2^2\ln\frac{\bar\mu^2}{m_H^2}\right)+(\lambda_3+\lambda_4-\lambda_5)\left(m_A^2+\mu_2^2\ln\frac{\bar\mu^2}{m_A^2}\right)\right],$$

$$\lambda_1(\bar\mu)\simeq\frac{g_2^2m_h^2}{8m_W^2}+\frac{1}{64\pi^2}\left[2\lambda_3^2\ln\frac{\bar\mu^2}{m_{H_\pm}^2}-12h_t^4\ln\frac{\bar\mu^2}{m_t^2}\right. \tag{C.33}$$
$$\left.+(\lambda_3+\lambda_4+\lambda_5)^2\ln\frac{\bar\mu^2}{m_H^2}+(\lambda_3+\lambda_4-\lambda_5)^2\ln\frac{\bar\mu^2}{m_A^2}\right].$$

Apart from directly approximating eqs. (C.25) and (C.26), these expressions can also be derived from the "naive" procedure of minimizing the effective potential V_0+V_1, and tuning $\mu_1^2(m_Z)$ and $\lambda_1(m_Z)$ so that the location of the minimum is at $v_{\rm min}^2\simeq 4m_W^2/g_2^2$ and the second derivative at the minimum is $(V_0+V_1)''(v_{\rm min})\simeq m_h^2$. This naive procedure can easily be implemented numerically and then also applied to the 2-loop potential at zero temperature.

C.4. Practical procedure

A problem with the 1-loop expressions listed in appendix C.3 is that if the couplings λ_3,λ_4 and λ_5 are first determined at tree level, and these values are subsequently inserted into the 1-loop corrections, as given in eqs. (C.25)–(C.31), then the corrections are in many cases of order 100%; for instance, $\lambda_1(m_Z)$ can be driven to a negative value. If corrections are of order 100%, there is no reason to trust the results. The problem can be somewhat "regulated" by solving eqs. (C.25)–(C.31) "self-consistently", i.e. by requiring that the couplings have the same values on both sides of the equations. In general, this reduces the magnitude of the largest coupling

λ_3, whereby the corrections remain below 100%. A further "resummation" can be implemented by determining $\mu_1^2(m_Z)$ and $\lambda_1(m_Z)$ *à la* Coleman–Weinberg, as outlined below eq. (C.33). An advantage of this procedure is that 2-loop corrections can be partially included into $\mu_1^2(m_Z)$ and $\lambda_1(m_Z)$. The values listed in Table 3 have been obtained by determining $\mu_1^2(m_Z)$ and $\lambda_1(m_Z)$ from the effective potential and the other parameters from the 1-loop pole mass relations in sec. C.3. However, we have also tested the procedure where 1-loop pole mass relations are used for all the couplings. This changes the values of $\mu_1^2(m_Z)$ and $\lambda_1(m_Z)$ given in Table 3 by up to $\sim 20\%$ for BM2, and only a few % for BM1 and BM3, however our conclusions concerning thermal effects remain unchanged in all cases.

C.5. Counterterms and renormalization group equations

Finally, let us list the counterterms needed in our analysis. The notation for them was defined in sec. 4.2. We stress that the same counterterms appear both in the vacuum renormalization computations of the current section and in the thermal 2-loop effective potential given in Appendix B. The results agree with ref. [14] for the counterterms that can be found there. The complete list reads

$$\delta Z_{\mu_1^2} = \frac{1}{(4\pi)^2\epsilon}\left[3h_t^2 - \frac{9g_2^2}{4} + 6\lambda_1 + \frac{\mu_2^2}{\mu_1^2}(2\lambda_3+\lambda_4)\right], \tag{C.34}$$

$$\delta Z_{\mu_2^2} = \frac{1}{(4\pi)^2\epsilon}\left[-\frac{9g_2^2}{4} + 6\lambda_2 + \frac{\mu_1^2}{\mu_2^2}(2\lambda_3+\lambda_4)\right], \tag{C.35}$$

$$\delta Z_{\lambda_1} = \frac{1}{(4\pi)^2\epsilon}\left[6h_t^2 - \frac{9g_2^2}{2} + \frac{9g_2^4}{16\lambda_1} - \frac{3h_t^4}{\lambda_1} + 12\lambda_1 + \frac{2\lambda_3^2+2\lambda_3\lambda_4+\lambda_4^2+\lambda_5^2}{2\lambda_1}\right], \tag{C.36}$$

$$\delta Z_{\lambda_2} = \frac{1}{(4\pi)^2\epsilon}\left[-\frac{9g_2^2}{2} + \frac{9g_2^4}{16\lambda_2} + 12\lambda_2 + \frac{2\lambda_3^2+2\lambda_3\lambda_4+\lambda_4^2+\lambda_5^2}{2\lambda_2}\right], \tag{C.37}$$

$$\delta Z_{\lambda_3} = \frac{1}{(4\pi)^2\epsilon}\left[3h_t^2 - \frac{9g_2^2}{2} + \frac{9g_2^4}{8\lambda_3} + 6(\lambda_1+\lambda_2) + 2\lambda_3 + \frac{2(\lambda_1+\lambda_2)\lambda_4+\lambda_4^2+\lambda_5^2}{\lambda_3}\right], \tag{C.38}$$

$$\delta Z_{\lambda_4} = \frac{1}{(4\pi)^2\epsilon}\left[3h_t^2 - \frac{9g_2^2}{2} + 2(\lambda_1+\lambda_2) + 4\lambda_3 + 2\lambda_4 + \frac{4\lambda_5^2}{\lambda_4}\right], \tag{C.39}$$

$$\delta Z_{\lambda_5} = \frac{1}{(4\pi)^2\epsilon}\left[3h_t^2 - \frac{9g_2^2}{2} + 2(\lambda_1+\lambda_2) + 4\lambda_3 + 6\lambda_4\right], \tag{C.40}$$

$$\delta Z_{g_2^2} = \frac{g_2^2}{(4\pi)^2\epsilon}\left[\frac{4n_G}{3} - 7\right], \tag{C.41}$$

$$\delta Z_{g_3^2} = \frac{g_3^2}{(4\pi)^2\epsilon}\left[\frac{4n_G}{3} - 11\right], \tag{C.42}$$

$$\delta Z_{h_t^2} = \frac{1}{(4\pi)^2\epsilon}\left[\frac{9h_t^2}{2} - \frac{9g_2^2}{4} - 8g_3^2\right], \tag{C.43}$$

$$\delta Z_{\phi} = \frac{1}{(4\pi)^2\epsilon}\left[-3h_t^2 + 3g_2^2\right], \tag{C.44}$$

$$\delta Z_v = \frac{1}{(4\pi)^2\epsilon}\left[3h_t^2 + \frac{5g_2^2}{2}\right], \tag{C.45}$$

$$\delta Z_\chi = \frac{1}{(4\pi)^2\epsilon}\left[\frac{3g_2^2}{2}\right], \tag{C.46}$$

$$\delta Z_A = \delta Z_\xi \;=\; \frac{g_2^2}{(4\pi)^2\epsilon}\left[3 - \frac{4n_G}{3}\right]. \tag{C.47}$$

The counterterm δZ_χ, appearing in eq. (B.3), only contributes to thermal effects which are formally of higher order than the accuracy of the computation.

As usual, the counterterms fix the renormalization group equations as

$$\bar{\mu}\frac{\mathrm{d}\lambda_i}{\mathrm{d}\bar{\mu}} \;=\; 2\lambda_i\,\epsilon\,\delta Z_{\lambda_i} + \mathcal{O}(\lambda_i^3)\,, \tag{C.48}$$

and similarly for the other couplings.

References

[1] N.G. Deshpande, E. Ma, Pattern of symmetry breaking with two Higgs doublets, Phys. Rev. D 18 (1978) 2574.
[2] E. Ma, Verifiable radiative seesaw mechanism of neutrino mass and dark matter, Phys. Rev. D 73 (2006) 077301, arXiv:hep-ph/0601225.
[3] R. Barbieri, L.J. Hall, V.S. Rychkov, Improved naturalness with a heavy Higgs: an alternative road to LHC physics, Phys. Rev. D 74 (2006) 015007, arXiv:hep-ph/0603188.
[4] L. Lopez Honorez, E. Nezri, J.F. Oliver, M.H.G. Tytgat, The inert doublet model: an archetype for dark matter, J. Cosmol. Astropart. Phys. 02 (2007) 028, arXiv:hep-ph/0612275.
[5] M. Gustafsson, E. Lundström, L. Bergström, J. Edsjö, Significant gamma lines from inert Higgs dark matter, Phys. Rev. Lett. 99 (2007) 041301, arXiv:astro-ph/0703512.
[6] T. Hambye, M.H.G. Tytgat, Electroweak symmetry breaking induced by dark matter, Phys. Lett. B 659 (2008) 651, arXiv:0707.0633.
[7] P. Agrawal, E.M. Dolle, C.A. Krenke, Signals of inert doublet dark matter in neutrino telescopes, Phys. Rev. D 79 (2009) 015015, arXiv:0811.1798.
[8] S. Andreas, M.H.G. Tytgat, Q. Swillens, Neutrinos from inert doublet dark matter, J. Cosmol. Astropart. Phys. 04 (2009) 004, arXiv:0901.1750.
[9] T. Hambye, F.-S. Ling, L. Lopez Honorez, J. Rocher, Scalar multiplet dark matter, J. High Energy Phys. 07 (2009) 090, arXiv:0903.4010;
T. Hambye, F.-S. Ling, L. Lopez Honorez, J. Rocher, J. High Energy Phys. 05 (2010) 066 (Erratum).
[10] C. Arina, F.-S. Ling, M.H.G. Tytgat, The inert doublet model and inelastic dark matter, J. Cosmol. Astropart. Phys. 10 (2009) 018, arXiv:0907.0430.
[11] E.M. Dolle, S. Su, The inert dark matter, Phys. Rev. D 80 (2009) 055012, arXiv:0906.1609.
[12] L. Lopez Honorez, C.E. Yaguna, The inert doublet model of dark matter revisited, J. High Energy Phys. 09 (2010) 046, arXiv:1003.3125.
[13] L. Lopez Honorez, C.E. Yaguna, A new viable region of the inert doublet model, J. Cosmol. Astropart. Phys. 01 (2011) 002, arXiv:1011.1411.
[14] A. Goudelis, B. Herrmann, O. Stål, Dark matter in the inert doublet model after the discovery of a Higgs-like boson at the LHC, J. High Energy Phys. 09 (2013) 106, arXiv:1303.3010.
[15] C. Garcia-Cely, A. Ibarra, Novel gamma-ray spectral features in the inert doublet model, J. Cosmol. Astropart. Phys. 09 (2013) 025, arXiv:1306.4681.
[16] M. Klasen, C.E. Yaguna, J.D. Ruiz-Álvarez, Electroweak corrections to the direct detection cross section of inert Higgs dark matter, Phys. Rev. D 87 (2013) 075025, arXiv:1302.1657.
[17] A. Arhrib, Y.L.S. Tsai, Q. Yuan, T.C. Yuan, An updated analysis of inert Higgs doublet model in light of the recent results from LUX, PLANCK, AMS-02 and LHC, J. Cosmol. Astropart. Phys. 06 (2014) 030, arXiv:1310.0358.
[18] K.P. Modak, D. Majumdar, Confronting galactic and extragalactic γ-rays observed by Fermi-lat with annihilating dark matter in an inert Higgs doublet model, Astrophys. J. Suppl. 219 (2015) 37, arXiv:1502.05682.

[19] F.S. Queiroz, C.E. Yaguna, The CTA aims at the inert doublet model, J. Cosmol. Astropart. Phys. 02 (2016) 038, arXiv:1511.05967.
[20] C. Garcia-Cely, M. Gustafsson, A. Ibarra, Probing the inert doublet dark matter model with Cherenkov telescopes, J. Cosmol. Astropart. Phys. 02 (2016) 043, arXiv:1512.02801.
[21] S. Banerjee, N. Chakrabarty, A revisit to scalar dark matter with radiative corrections, arXiv:1612.01973.
[22] A. Barroso, P.M. Ferreira, I.P. Ivanov, R. Santos, Metastability bounds on the two Higgs doublet model, J. High Energy Phys. 06 (2013) 045, arXiv:1303.5098.
[23] N. Chakrabarty, D.K. Ghosh, B. Mukhopadhyaya, I. Saha, Dark matter, neutrino masses and high scale validity of an inert Higgs doublet model, Phys. Rev. D 92 (2015) 015002, arXiv:1501.03700.
[24] N. Khan, S. Rakshit, Constraints on inert dark matter from the metastability of the electroweak vacuum, Phys. Rev. D 92 (2015) 055006, arXiv:1503.03085.
[25] B. Swiezewska, Inert scalars and vacuum metastability around the electroweak scale, J. High Energy Phys. 07 (2015) 118, arXiv:1503.07078.
[26] P.M. Ferreira, B. Swiezewska, One-loop contributions to neutral minima in the inert doublet model, J. High Energy Phys. 04 (2016) 099, arXiv:1511.02879.
[27] E. Lundström, M. Gustafsson, J. Edsjö, The inert doublet model and LEP II limits, Phys. Rev. D 79 (2009) 035013, arXiv:0810.3924.
[28] E. Dolle, X. Miao, S. Su, B. Thomas, Dilepton signals in the inert doublet model, Phys. Rev. D 81 (2010) 035003, arXiv:0909.3094.
[29] M. Gustafsson, S. Rydbeck, L. Lopez-Honorez, E. Lundström, Status of the inert doublet model and the role of multileptons at the LHC, Phys. Rev. D 86 (2012) 075019, arXiv:1206.6316.
[30] A. Arhrib, R. Benbrik, N. Gaur, $H \to \gamma\gamma$ in inert Higgs doublet model, Phys. Rev. D 85 (2012) 095021, arXiv:1201.2644.
[31] M. Krawczyk, D. Sokolowska, P. Swaczyna, B. Swiezewska, Constraining inert dark matter by $R_{\gamma\gamma}$ and WMAP data, J. High Energy Phys. 09 (2013) 055, arXiv:1305.6266.
[32] G.C. Dorsch, S.J. Huber, K. Mimasu, J.M. No, Echoes of the electroweak phase transition: discovering a second Higgs doublet through $A_0 \to Z H_0$, Phys. Rev. Lett. 113 (2014) 211802, arXiv:1405.5537.
[33] G. Belanger, B. Dumont, A. Goudelis, B. Herrmann, S. Kraml, D. Sengupta, Dilepton constraints in the inert doublet model from run 1 of the LHC, Phys. Rev. D 91 (2015) 115011, arXiv:1503.07367.
[34] A. Arhrib, R. Benbrik, J. El Falaki, A. Jueid, Radiative corrections to the triple Higgs coupling in the inert Higgs doublet model, J. High Energy Phys. 12 (2015) 007, arXiv:1507.03630.
[35] A. Ilnicka, M. Krawczyk, T. Robens, Inert doublet model in the light of LHC Run I and astrophysical data, Phys. Rev. D 93 (2016) 055026, arXiv:1508.01671.
[36] N. Blinov, J. Kozaczuk, D.E. Morrissey, A. de la Puente, Compressing the inert doublet model, Phys. Rev. D 93 (2016) 035020, arXiv:1510.08069.
[37] M.A. Díaz, B. Koch, S. Urrutia-Quiroga, Constraints to dark matter from inert Higgs doublet model, Adv. High Energy Phys. 2016 (2016) 8278375, arXiv:1511.04429.
[38] M. Hashemi, M. Krawczyk, S. Najjari, A.F. Zarnecki, Production of inert scalars at the high energy e^+e^- colliders, J. High Energy Phys. 02 (2016) 187, arXiv:1512.01175.
[39] P. Poulose, S. Sahoo, K. Sridhar, Exploring the inert doublet model through the dijet plus missing transverse energy channel at the LHC, Phys. Lett. B 765 (2017) 300, arXiv:1604.03045.
[40] S. Kanemura, M. Kikuchi, K. Sakurai, Testing the dark matter scenario in the inert doublet model by future precision measurements of the Higgs boson couplings, Phys. Rev. D 94 (2016) 115011, arXiv:1605.08520.
[41] A. Datta, N. Ganguly, N. Khan, S. Rakshit, Exploring collider signatures of the inert Higgs doublet model, Phys. Rev. D 95 (2017) 015017, arXiv:1610.00648.
[42] M. Hashemi, S. Najjari, Observability of inert scalars at the LHC, arXiv:1611.07827.
[43] A. Belyaev, G. Cacciapaglia, I.P. Ivanov, F. Rojas, M. Thomas, Anatomy of the inert two Higgs doublet model in the light of the LHC and non-LHC dark matter searches, arXiv:1612.00511.
[44] I.F. Ginzburg, K.A. Kanishev, M. Krawczyk, D. Sokolowska, Evolution of universe to the present inert phase, Phys. Rev. D 82 (2010) 123533, arXiv:1009.4593.
[45] T.A. Chowdhury, M. Nemevsek, G. Senjanovic, Y. Zhang, Dark matter as the trigger of strong electroweak phase transition, J. Cosmol. Astropart. Phys. 02 (2012) 029, arXiv:1110.5334.
[46] D. Borah, J.M. Cline, Inert doublet dark matter with strong electroweak phase transition, Phys. Rev. D 86 (2012) 055001, arXiv:1204.4722.
[47] G. Gil, P. Chankowski, M. Krawczyk, Inert dark matter and strong electroweak phase transition, Phys. Lett. B 717 (2012) 396, arXiv:1207.0084.

[48] J.M. Cline, K. Kainulainen, Improved electroweak phase transition with subdominant inert doublet dark matter, Phys. Rev. D 87 (2013) 071701, arXiv:1302.2614.
[49] N. Blinov, J. Kozaczuk, D.E. Morrissey, C. Tamarit, Electroweak baryogenesis from exotic electroweak symmetry breaking, Phys. Rev. D 92 (2015) 035012, arXiv:1504.05195.
[50] N. Blinov, S. Profumo, T. Stefaniak, The electroweak phase transition in the inert doublet model, J. Cosmol. Astropart. Phys. 07 (2015) 028, arXiv:1504.05949.
[51] P. Basler, M. Krause, M. Mühlleitner, J. Wittbrodt, A. Wlotzka, Strong first order electroweak phase transition in the CP-conserving 2HDM revisited, arXiv:1612.04086.
[52] M. Laine, K. Rummukainen, What's new with the electroweak phase transition?, Nucl. Phys. B, Proc. Suppl. 73 (1999) 180, arXiv:hep-lat/9809045.
[53] P. Ginsparg, First and second order phase transitions in gauge theories at finite temperature, Nucl. Phys. B 170 (1980) 388.
[54] T. Appelquist, R.D. Pisarski, High-temperature Yang–Mills theories and three-dimensional Quantum Chromodynamics, Phys. Rev. D 23 (1981) 2305.
[55] K. Kajantie, M. Laine, K. Rummukainen, M.E. Shaposhnikov, Generic rules for high temperature dimensional reduction and their application to the Standard Model, Nucl. Phys. B 458 (1996) 90, arXiv:hep-ph/9508379.
[56] D. Land, E.D. Carlson, Two stage phase transition in two Higgs models, Phys. Lett. B 292 (1992) 107, arXiv:hep-ph/9208227.
[57] A. Hammerschmitt, J. Kripfganz, M.G. Schmidt, Baryon asymmetry from a two stage electroweak phase transition?, Z. Phys. C 64 (1994) 105, arXiv:hep-ph/9404272.
[58] M.E. Shaposhnikov, Baryon asymmetry of the universe in standard electroweak theory, Nucl. Phys. B 287 (1987) 757.
[59] M. Laine, K. Rummukainen, Two Higgs doublet dynamics at the electroweak phase transition: a nonperturbative study, Nucl. Phys. B 597 (2001) 23, arXiv:hep-lat/0009025.
[60] M. Laine, G. Nardini, K. Rummukainen, Lattice study of an electroweak phase transition at $m_h \sim 126$ GeV, J. Cosmol. Astropart. Phys. 01 (2013) 011, arXiv:1211.7344.
[61] M. Laine, M. Meyer, Standard Model thermodynamics across the electroweak crossover, J. Cosmol. Astropart. Phys. 07 (2015) 035, arXiv:1503.04935.
[62] M. D'Onofrio, K. Rummukainen, Standard Model cross-over on the lattice, Phys. Rev. D 93 (2016) 025003, arXiv:1508.07161.
[63] T. Brauner, T.V.I. Tenkanen, A. Tranberg, A. Vuorinen, D.J. Weir, Dimensional reduction of the standard model coupled to a new singlet scalar field, J. High Energy Phys. 03 (2017) 007, arXiv:1609.06230.
[64] M. Laine, M. Losada, Two loop dimensional reduction and effective potential without temperature expansions, Nucl. Phys. B 582 (2000) 277, arXiv:hep-ph/0003111.
[65] K. Funakubo, E. Senaha, Two-loop effective potential, thermal resummation, and first-order phase transitions: beyond the high-temperature expansion, Phys. Rev. D 87 (2013) 054003, arXiv:1210.1737.
[66] W. Buchmüller, Z. Fodor, A. Hebecker, Gauge invariant treatment of the electroweak phase transition, Phys. Lett. B 331 (1994) 131, arXiv:hep-ph/9403391.
[67] M. D'Onofrio, K. Rummukainen, A. Tranberg, The sphaleron rate in the minimal standard model, Phys. Rev. Lett. 113 (2014) 141602, arXiv:1404.3565.
[68] M. Garny, T. Konstandin, On the gauge dependence of vacuum transitions at finite temperature, J. High Energy Phys. 07 (2012) 189, arXiv:1205.3392.
[69] G.D. Moore, K. Rummukainen, Electroweak bubble nucleation, nonperturbatively, Phys. Rev. D 63 (2001) 045002, arXiv:hep-ph/0009132.
[70] M. Laine, Gauge dependence of the high-temperature two-loop effective potential for the Higgs field, Phys. Rev. D 51 (1995) 4525, arXiv:hep-ph/9411252.
[71] J. Kripfganz, A. Laser, M.G. Schmidt, The high-temperature two-loop effective potential of the electroweak theory in a general 't Hooft background gauge, Phys. Lett. B 351 (1995) 266, arXiv:hep-ph/9501317.
[72] M.E. Carrington, The effective potential at finite temperature in the Standard Model, Phys. Rev. D 45 (1992) 2933.
[73] P.B. Arnold, O. Espinosa, The effective potential and first order phase transitions: beyond leading order, Phys. Rev. D 47 (1993) 3546, arXiv:hep-ph/9212235;
P.B. Arnold, O. Espinosa, Phys. Rev. D 50 (1994) 6662 (Erattum).
[74] R.R. Parwani, Resummation in a hot scalar field theory, Phys. Rev. D 45 (1992) 4695, arXiv:hep-ph/9204216;
R.R. Parwani, Phys. Rev. D 48 (1993) 5965 (Erratum).
[75] W. Buchmüller, T. Helbig, D. Walliser, First order phase transitions in scalar electrodynamics, Nucl. Phys. B 407 (1993) 387.

[76] F. Karsch, A. Patkós, P. Petreczky, Screened perturbation theory, Phys. Lett. B 401 (1997) 69, arXiv:hep-ph/9702376.
[77] S. Chiku, T. Hatsuda, Optimized perturbation theory at finite temperature, Phys. Rev. D 58 (1998) 076001, arXiv:hep-ph/9803226.
[78] J.O. Andersen, E. Braaten, M. Strickland, Screened perturbation theory to three loops, Phys. Rev. D 63 (2001) 105008, arXiv:hep-ph/0007159.
[79] M. Dine, R.G. Leigh, P.Y. Huet, A.D. Linde, D.A. Linde, Towards the theory of the electroweak phase transition, Phys. Rev. D 46 (1992) 550, arXiv:hep-ph/9203203.
[80] M. Sperling, D. Stöckinger, A. Voigt, Renormalization of vacuum expectation values in spontaneously broken gauge theories, J. High Energy Phys. 07 (2013) 132, arXiv:1305.1548.
[81] M. Sperling, D. Stöckinger, A. Voigt, Renormalization of vacuum expectation values in spontaneously broken gauge theories: two-loop results, J. High Energy Phys. 01 (2014) 068, arXiv:1310.7629.
[82] A. Sirlin, Radiative corrections in the $\mathrm{SU}(2)_L \times \mathrm{U}(1)$ theory: a simple renormalization framework, Phys. Rev. D 22 (1980) 971.
[83] H.K. Guo, Y.Y. Li, T. Liu, M. Ramsey-Musolf, J. Shu, Lepton-flavored electroweak baryogenesis, arXiv:1609.09849.
[84] C. Ford, I. Jack, D.R.T. Jones, The Standard Model effective potential at two loops, Nucl. Phys. B 387 (1992) 373, arXiv:hep-ph/0111190;
C. Ford, I. Jack, D.R.T. Jones, Nucl. Phys. B 504 (1997) 551 (Erattum).
[85] A.I. Davydychev, J.B. Tausk, Two loop selfenergy diagrams with different masses and the momentum expansion, Nucl. Phys. B 397 (1993) 123.
[86] M. Caffo, H. Czyz, S. Laporta, E. Remiddi, The Master differential equations for the two loop sunrise selfmass amplitudes, Nuovo Cimento A 111 (1998) 365, arXiv:hep-th/9805118.
[87] P.B. Arnold, C.-X. Zhai, The three-loop free energy for pure gauge QCD, Phys. Rev. D 50 (1994) 7603, arXiv:hep-ph/9408276.
[88] P.B. Arnold, C.-X. Zhai, The three-loop free energy for high-temperature QED and QCD with fermions, Phys. Rev. D 51 (1995) 1906, arXiv:hep-ph/9410360.
[89] M. Nishimura, Y. Schröder, IBP methods at finite temperature, J. High Energy Phys. 09 (2012) 051, arXiv:1207.4042.